AD-A066 200 AIR FORCE INST OF TECH WRIGHT-PATTERSON AFB OHIO SCH--ETC F/G 18/12
ISOTOPIC CORRELATION TECHNIQUES AS AN OFF-SITE REACTOR MONITOR.(U)
OCT 78 J L CLARK
UNCLASSIFIED AFIT/GNE/PH/78-12 NL

1 OF 2
AD A066200

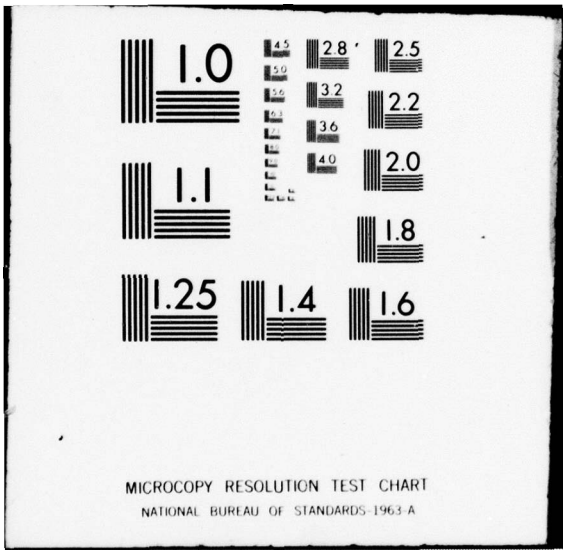
1.0
1.1
1.25
1.4
1.6
1.8
2.0
2.2
2.5
2.8
3.2
3.6
4.0
4.5
5.0
5.6
6.3
MICROCOPY RESOLUTION TEST CHART
NATIONAL BUREAU OF STANDARDS-1963-A

DISCLAIMER NOTICE

THIS DOCUMENT IS BEST QUALITY PRACTICABLE. THE COPY FURNISHED TO DDC CONTAINED A SIGNIFICANT NUMBER OF PAGES WHICH DO NOT REPRODUCE LEGIBLY.

(1)

(6) ISOTOPIC CORRELATION TECHNIQUES AS AN OFF-SITE REACTOR MONITOR

(9) Master's THESIS

(14) AFIT/GNE/PH/78-12

(10) James L. Clark Jr.
Capt. USMC

(11) Oct 78

(12) 103 p.

1413

Approved for public release; distribution unlimited

Ø12225

AFIT/GNE/PH/78-12

ISOTOPIC CORRELATION TECHNIQUES AS AN OFF-SITE REACTOR MONITOR

THESIS

Presented to the Faculty of the School of Engineering

of the Air Force Institute of Technology

Air University

in Partial Fulfillment of the

Requirements for the Degree of

Master of Science

By

James L. Clark Jr., B.S.

Captain USMC

Graduate Nuclear Effects

October 1978

PREFACE

I would like to express my appreciation to my advisors, Lt. David Hardin and Professor Richard Hagee, for their guidance in the development of this thesis.

A debt of gratitude is owed to Eleanor Bonsteel for her patience in typing this work.

J. L. Clark

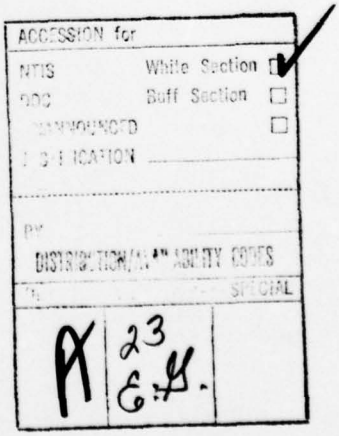

Contents

List of Figures

List of Tables

Abstract

The feasibility of using the mass ratio Nd146/Nd145 and the activity ratio Cs134/Cs137 as off-site indicators of bomb-grade plutonium production in commercial light water reactors is examined. The theoretical basis of these ratios as on-site indicators of fluence is developed and experimental validation of their utility as such is examined. The escape rate of cesium and neodymium is approximated and detection limits determined. Although both ratios are experimentally validated as indicators of fluence, neither cesium nor neodymium escapes a reactor in great enough concentration to be accurately measured off-site.

ISOTOPIC CORRELATION TECHNIQUES AS AN OFF-SITE REACTOR MONITOR

I. Introduction

The United States would like to export nuclear reactor technology and fuel without contributing to the proliferation of nuclear weapons. Prospective third world customers do not possess the technology to convert commercial uranium fuel to bomb-grade uranium; this requires an inversion of the ratio of U238/U235, which is 97/3 for a representative light water reactor (LWR) fuel. However, absorption of fast neutrons from fissioning U235 converts U238 into Pu239. Pu239 has nuclear properties similar to those of U235; it can be used as reactor fuel or weapon fuel. The continuous conversion of U238 to Pu239 in a power reactor burning U235 is the proliferation concern.

If the Pu239 is not removed from the reactor core soon after its formation, it too absorbs neutrons and is converted to Pu240. Substantial amounts of Pu240 in a mixture of the two plutonium isotopes makes the plutonium unusable in a weapon; moreover, the separation of these isotopes is even more difficult than the enrichment of uranium. Economical generation of power requires a long, sustained fission cycle; production of bomb-grade plutonium, hereafter referred to as Pu239 isolation, requires frequent

shutdown for Pu239 removal. Obviously, on-site inspection to determine length of fission cycle is the most straightforward method for determining whether a reactor is being used for production of power or Pu239 isolation.

Another method for determining Pu239 isolation involves examination of irradiated fuel elements. Weitkamp has demonstrated a linear relationship between U235 depletion and the ratio Pu240/Pu239 (Ref 1:212). Data generated by Origen, the Oak Ridge National Laboratories Isotope Generation and Depletion Code, verifies this relationship; U235 depletion and the ratio Pu240/Pu239 have a linear correlation factor of 0.9995 (Ref 2:106). Determination of U235 depletion, or burnup, of a fuel element indicates the relative amounts of Pu240 and Pu239; low burnup infers Pu239 isolation. One method of determining fuel burnup is called isotopic correlation techniques (ICT); it is based on the fact that the ratio of certain fission product nuclides varies systematically with fuel burnup. Use of a ratio eliminates the need for knowledge of the original fuel mass.

ICT have demonstrated their utility as an on-site safeguards technique for determining Pu239 isolation; they are also used at fuel recycling facilities to verify fissile content of incoming shipments. The problem addressed herein is the feasibility of using isotopic correlation techniques to monitor, off-site, for production of bomb-grade plutonium in a power reactor.

Goodwin, dealing with the same prob lem, developed a set of criteria which a nuclide ratio must meet if off-site application of ICT is to be possible (Ref 3:10). The essential elements of those criteria are:

(1) The nuclides must be isotopes of the same element.

(2) This element's chemical properties must enable it to escape from the fuel and reactor.

(3) The istopic ratio must be measurable off-site.

Goodwin predicts that in 1982, 75% of the world's reactors will be LWR's, and that 92% of the world's reactors will be using slightly enriched (1-3%) uranium dioxide (Ref 3:13,15). Only LWR's burning slightly enriched uranium dioxide will be considered.

Isotopic correlations have been the subject of both theoretical and experimental investigation (Ref 4:426). Theoretical investigation is generally carried out by performing accurate burnup calculations, from which correlations are derived. Experimental investigation is based on detailed measurement of irradiated fuel isotopic composition, from which correlations are derived.

Analysis of the off-site application of ICT began with a literature survey of theoretical correlation investigations. Isotopic ratios thereby identified were evaluated against Goodwin's criteria; the ratios Cs134/Cs137 and Nd146/Nd145 were judged suitable. A literature survey of experimental investigations of these two ratios was

conducted to validate them as indicators of fuel depletion. The literature revealed a power history dependence of the cesium ratio, but the degree of this dependence and its impact on the utility of the cesium ratio as a burnup indicator, independent of knowledge about power history, were not clear. Calculations were performed to determine the degree and impact of this dependence. The escape mechanisms from fuel to environment were examined and escape rates estimated. These escape rates were coupled to the dilution processes operating on the two reactor effluents considered, stack gas and coolant water, and limits of ratio measurability predicted.

II. Theoretical Analysis of ICT

The evolution of isotopic correlation techniques began with W. J. Maeck's proposal, in 1965, that ratios of fission product nuclides be used for determination of nuclear fuel burnup (Ref 5). At that time, determination of burnup by fission product analysis was based on the quantitative measurement of a selected fission product nuclide. Use of a ratio instead of an absolute atom abundance circumvented the requirements for complete sample dissolution and volume measurements.

Maeck's method was based on the premise that for stable fission product A, with large capture cross section, and stable fission product A+1, with small capture cross section, the ratio A+1/A increases exponentially with irradiation time. His calculations indicated that the ratios Nd144/Nd143, Kr84/Kr83, and Xe132/Xe131 were suitable for burnup determination.

The first interest in radionuclide ratios as indicators of fuel burnup was demonstrated in 1968 by Hick and Lammer (Ref 6). They developed a computer code, IRREL, for calculation of fission product activities as a function of fluence and determined that the activity ratio Cs134/Cs137 was an effective measure of fluence. Fluence is a measure of fuel exposure; fuel depletion

is easily calculated from the relationships:

$$N^{U}_{235} = N^{U}_{(0)235}\, e^{-(\sigma_a \Phi)} \qquad (1)$$

$$U235\ \text{DEPLETION} = \left(N^{U}_{(0)235} - N^{U}_{235}\right) / N^{U}_{(0)235} \qquad (2)$$

where

$N^{U}_{(0)235}$ = initial amount of U235

N^{U}_{235} = amount of U235 at fluence Φ

σ_a = absorption cross section or U235

Φ = fluence

The most complete compilation of isotopic ratios for LWR fuels is that of the Joint Research Center of Euratom (Ref 4:427). They identify the following ratios as indicators of U235 depletion: Cs134/Cs137, Kr84/Kr86, Kr86/Kr83, Kr84/Kr83, Xe132/Xe131, Xe134/Xe131, Xe132/Xe134, Nd146/Nd145, Nd146/Nd148, Nd148/Nd145. Two ratios of neodymium isotopes identified by Maeck (Ref 5:15) are ignored in the preceding compilation; they are Nd144/Nd143 and Nd146/Nd143. These twelve ratios meet the first of Goodwin's criteria. Their escape potential and off-site measurability must be determined. Since escape potential is determined by chemical characteristics, use of same-

element ratios simplifies escape-path analysis. The important determinants of escape potential are state (solid, liquid, gas) and chemical reactivity. Escape potential increases as state changes from solid to gas and decreases as reactivity increases.

Krypton and xenon are inert gases; their escape potential is extremely high. However, all their isotopes of interest herein are naturally occurring. Kr83 and Xe131 have isomeric states, but the half-life of Kr83m is less than two hours and only 8E-3(i.e. 8×10^{-3}) of the Xe131 passes through the isomeric state (Ref 7). Disregarding these isometric states, calculations were performed to compare expected effluent concentrations of the three krypton isotopes and the three xenon isotopes to environmental background concentrations. Using data from the BWR at Oyster Creek, N. J., it was determined that the stack gas contained concentrations on the order of 1E6 per cc of the Krypton isotopes and 1E7 per cc of the Xenon isotopes. The atmospheric background concentrations were calculated to be on the order of 1E12 per cc for krypton isotopes and 1E11 for xenon isotopes. These calculations are contained in Appendix A. Krypton and xenon are not present in measurable amount in coolant water effluent. Clearly, krypton and xenon do not meet the off-site measurability criteria; they will not be considered further.

The escape potential of the neodymium isotopes would appear to be low; neodymium is a non-volatile reactive rare-earth metal. Its melting point is 1024 degrees (centigrade) and its boiling point is 3027 degrees (Ref 8:B 121). Escape data kept by reactor operators and agencies regulating them deal only with radionuclides (Ref 9). Of the neodymium isotopes of concern herein, only Nd144 is radioactive, but its half-life of 5E15 years causes its radioactivity to be commonly disregarded. As demonstrated in Appendix A, measured concentrations of one isotope can be used to infer concentrations of other isotopes of that element. The only indication of neodymium escape found in the literature was a Nd147 concentration of 3E-7 Curies per liter of coolant in a BWR (Ref 10:8). This activity concentration equates to a number density of 1.54E10 atoms of Nd147 per liter. Thermal-neutron fission of U235 results in the following yields:

6.03% Nd143, 5.62% Nd144, 3.98% Nd145,
3.07% Nd146, 2.70% Nd147, 1.71% Nd148

(Ref 11:98). All these isotopes could be expected to have been present in the coolant with concentrations of the same order of magnitude as Nd147.

Although 1E10 atoms per liter is certainly a measurable amount, neodymium's ability to escape from the coolant to the environment is uncertain. If neodymium does escape to the environment, its off-site measurability will be complicated by the natural occurrence of all isotopes of

interest (Ref 8:B51). Further consideration of neodymium's escape potential and off-site measurability is deferred until the analysis of escape mechanisms is completed. Since the neodymium ratios are, at this point, of questionable utility, experimental validation for only one of the ratios will be considered. In addition to being cited as an indicator of U235 depletion, the ratio Nd146/Nd145 shows a direct relationship to Pu240 content (Ref 1:212); only this neodymium ratio will be considered further.

The chemical characteristics of cesium do not immediately categorize its escape potential; although volatile (boiling point of 690 degrees), it is the most electropositive (reactive) element (Ref 8:B106). However, one environmental study has shown that Cs134 and Cs137 can be found in measurable concentrations in both the stack gas and discharge canal of a PWR (Ref 12). Since neither Cs134 nor Cs137 occur naturally (Ref 8:B46), off-site measurability will not be complicated by natural background concentrations. The cesium ratio appears to be the best candidate for off-site application.

The literature survey of theoretical investigations of ICT upon which the preceding selection of ratios was based revealed three other items of interest. The first of these items is the creation by the International Atomic Energy Agency (IAEA) of an ICT data bank; data has been collected from reprocessing plants and analytical laboratories and stored with a common format for ease of subse-

quent retrieval (Ref 13). The ratio chosen as an on-site indicator of U235 depletion was Cs134/Cs137. A code (ISOCORR) has been developed which performs the theoretical analysis of correlations and compares the calculated data with the experimental data stored in this bank(Ref 14).

The second item of interest is a wide concern over the sensitivity of theoretical isotopic correlations to fission product nuclear data (FPND) accuracies (Ref 1, 15-17). Weitkamp identifies the yield of Cs137 as the only significant FPND involved in the production scheme of Cs137 (Ref 17:201). He apparently disregards the short-lived precursors of Cs137 (I137 and Xe137). Weitkamp lists the yield and capture cross section of Cs133 and the capture cross section of Cs134 as the significant FPND in the production scheme of Cs134; again, he has disregarded the precursors of Cs133. As the uncertainties in cross sections are greater than the uncertainties in yields, the accuracy of the cross sections of Cs133 and Cs134 is the limiting factor in calculating a Cs134/Cs137 ratio. A 1% error in the cross section of Cs133 causes a 1% error in the amount of Cs134 (Ref 17:200). The important FPND in the calculation of the Nd146/Nd145 ratio are capture cross sections of Nd144, Nd145 and yields of Nd145, Nd146 (Ref 17:205).

The final item is an indirect reference to the power dependency of the Cs134/Cs137 ratio as a measure of fluence; this dependency was to become a concern during examination of the experimental investigations of ICT. Fig. 1 shows the

theoretical variation of the Cs^{134}/Cs^{137} activity ratio with irradiation time and neutron flux for fission of U235. The intersections of the flux and time lines are the plotted points. The two circled points both represent the same fluence; varying the flux by a factor of two changes the Cs^{134}/Cs^{137} ratio by 27%.

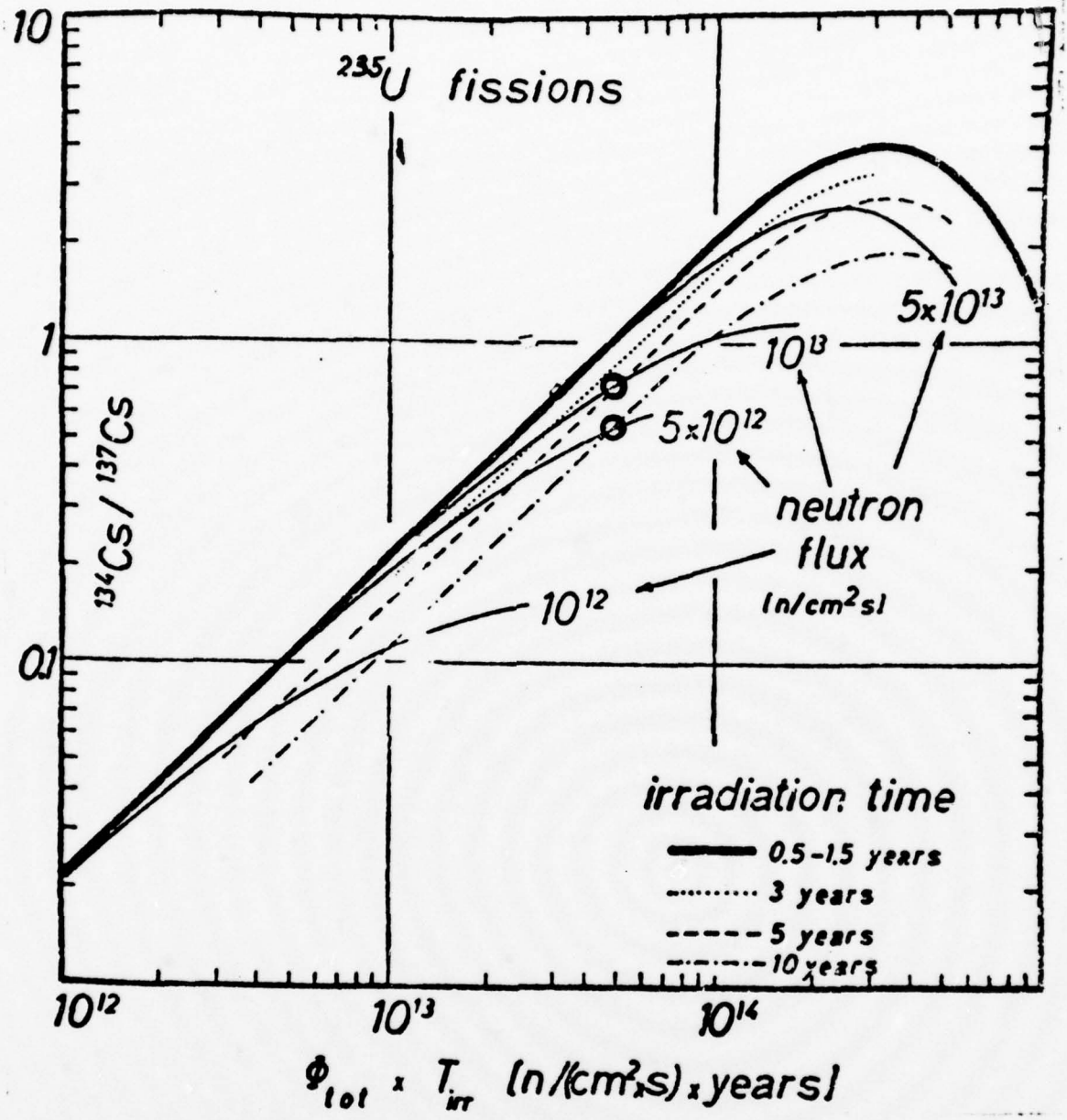

Fig. 1. Cs134/Cs137 Activity Ratio at Shutdown Versus Integrated Neutron Flux for Different values of Neutron Flux and Irradiation Time (Ref. 15:241)

III. Experimental Validation of Cesium and Neodymium Ratios

Selection of the ratios Cs134/Cs137 and Nd146/Nd145 as prospective off-site indicators of fuel burnup is based on their theoretical utility as on-site burnup indicators; experimental validation of their on-site utility was the subject of a second literature survey. The work of Hick and Lammer (Ref 18) demonstrates an interesting application of both the theoretical and experimental aspects of isotopic correlations; they combine gamma-spectrometric measurements and theoretical calculations to establish a fission product inventory which is more accurate and complete than is possible with either experiment or calculation alone. Their code (IRREL) for calculation of fission product inventory requires neutron flux input data (value and spectral shape) of unavailable accuracy. On the other hand, gamma-spectrometric measurements are sufficiently accurate for only a limited set of fission products; due to mutual line interference or absence of gamma lines, many isotopes cannot be measured accurately. Hick and Lammer use experimental results for Cs134 and Cs137 and a knowledge of the irradiation history to derive proper neutron flux input data for IRREL; IRREL then is able to compute a fission product inventory of any desired degree of completeness.

The relationship between fluence and fuel depletion is defined in the preceding chapter; another measure of fuel depletion, or burnup, is preferred in experimental work. This unit is the megawatt-day per tonne (MWD/T). As the name suggests, fuel in a reactor operating at a specific power level of one megawatt (thermal) per tonne (1000 Kilograms) of fuel initially present will be depleted by one MWD/T in one day. The fuel is considered to consist of heavy elements only; in fuel elements of uranium dioxide with stainless steel cladding, only the weight of the uranium dioxide is considered in the unit MWD/T (Ref 19:260).

Dragnev and Beets examine the feasibility of using non-destructive gamma spectrometry measurements of irradiated fuel assemblies to determine the type of fuel (pre-irradiation enrichment), the history of its irradiation, and the operational history of the reactor during the period when the measured fuel was in the core of the reactor (Ref 20). The irradiated fuel is from the German Vak reactor; the fuel elements are made of pellets with 1.27 cm outer diameter and 1.59 cm length. A fuel rod is composed of two 48-pellet sections; the rod diameter is 1.45 cm. The fuel consists of 2.33% enriched uranium in the form of sintered uranium dioxide; cladding is 0.85 mm Zircaloy-2.

Since it was planned to measure each fuel assembly in only one spot along its axis, measurements of the axial distribution of burnup are made to determine the best spot for measurement. The ratios between the intensities of the

605KeV gamma peak (Cs134) versus the 663 KeV peak (Cs137) and the 796 KeV peak (Cs134) versus the 663 KeV peak (Cs137) are used as burnup monitors. The results can be summarized as follows:

(1) The axial distributions of the activity ratios follow qualitatively the distribution of the integrated neutron flux at different points of the reactor core.

(2) The axial distribution of Cs134 activities decreases steeply to the ends of the fuel assemblies; this rapid decrease is caused by the fact that Cs134 accumulation is nearly proportional to the second degree of the integrated neutron flux.

(3) The activity ratio Cs134/Cs137 as a burnup monitor gives the correct burnup value despite the lack of fuel in the center of the rod (void between the two sections described above)

Fig. 2 shows the results of a single point measurement of the gamma spectrum of a Vak fuel assembly after 1.58 years cooling time. The peak labeled 605 is the 605 KeV peak of Cs134; the other peaks of interest are 662 (Cs137) and 796 (CS134, but mislabeled as Cs137). The quality of the figure is poor because it was duplicated from microfiche. The areas under the full-energy peaks are related to the amount of corresponding gamma radioactive fission products in the measured fuel assembly.

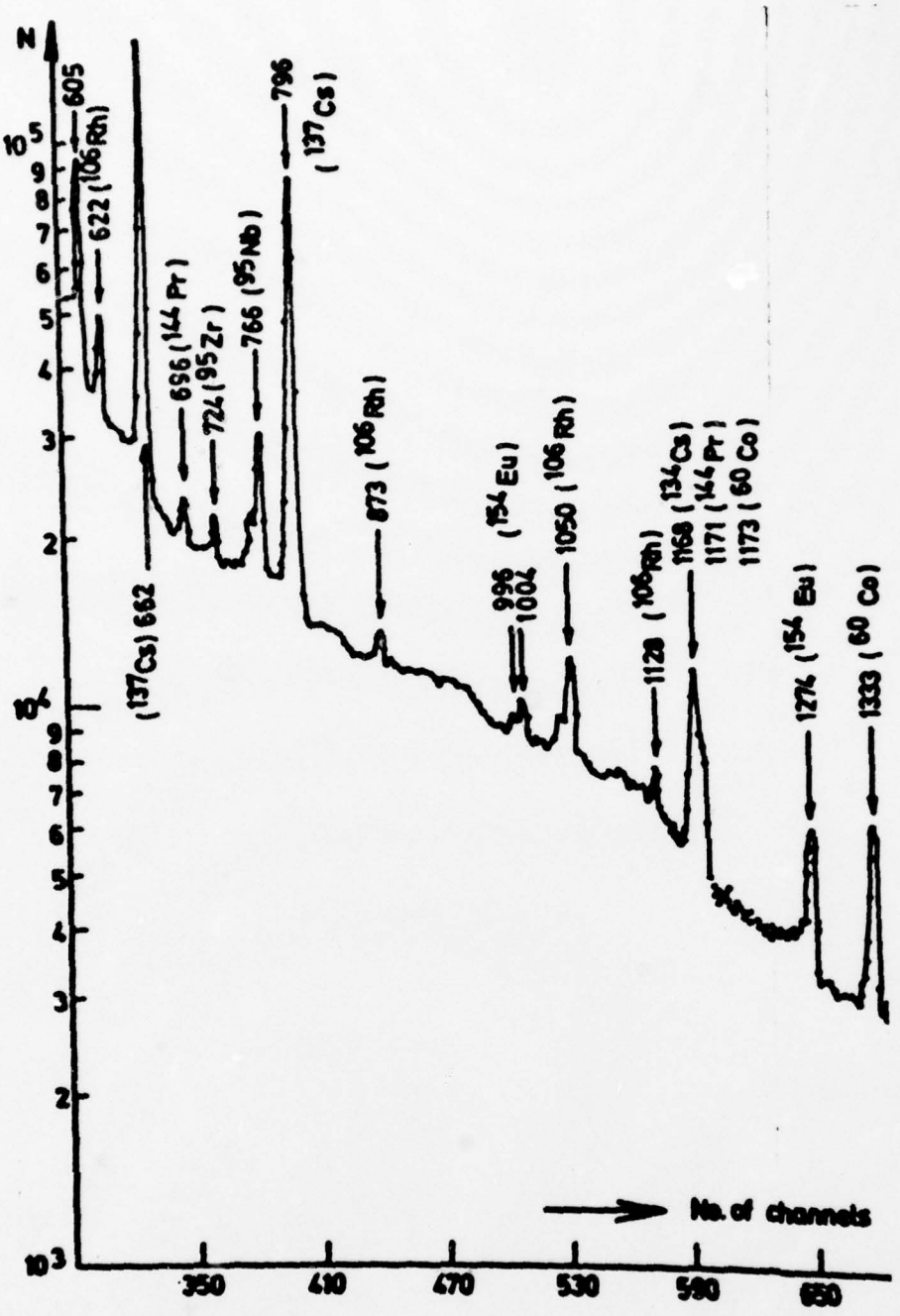

Fig. 2. Partial Gamma Spectrum for Vak Fuel Assembly (Ref. 20:34)

Single point measurements of the activity ratios Cs134(605 KeV)/Cs137 and Cs134 (796 KeV)/Cs137 for eleven Vak fuel assemblies with cooling time of 0.42 years are reported. Fig. 3 plots these measurements against the calculated burnup of each fuel assembly; the circled points represent the reported data. As the reported data represents a limited range of burnups, a linear least-squares fit of the data was calculated (Ref 21:43). The points marked by x represent a projection of this fit. The data associated with the 605 KeV peak has a linear correlation coefficient (R) of 0.737, while for the 796 KeV data, R=0.899.

Both the initial and final amounts of U235 for each fuel assembly are reported, permitting calculation of U235 depletion. Fig. 4 plots U235 depletion against the two activity ratios. Again, circled points represent reported data, and x's represent a least-squares fit. For the 605 KeV data, R=0.706; for the 796 KeV data, R=0.896.

Using the 796 KeV data, Dragnev and Beets formulated a method for making the Cs134/Cs137 ratio appear to be a far better indicator of burnup than demonstrated by Fig. 3. Their treatment involves dividing each activity ratio by the activity ratio of the fuel assembly with highest burnup, and dividing each burnup by the highest burnup; they calculate a linear correlation factor of 0.993 for the relationship between relative burnup and relative activity ratio.

Bresesti and Peroni report on experimental work corre-

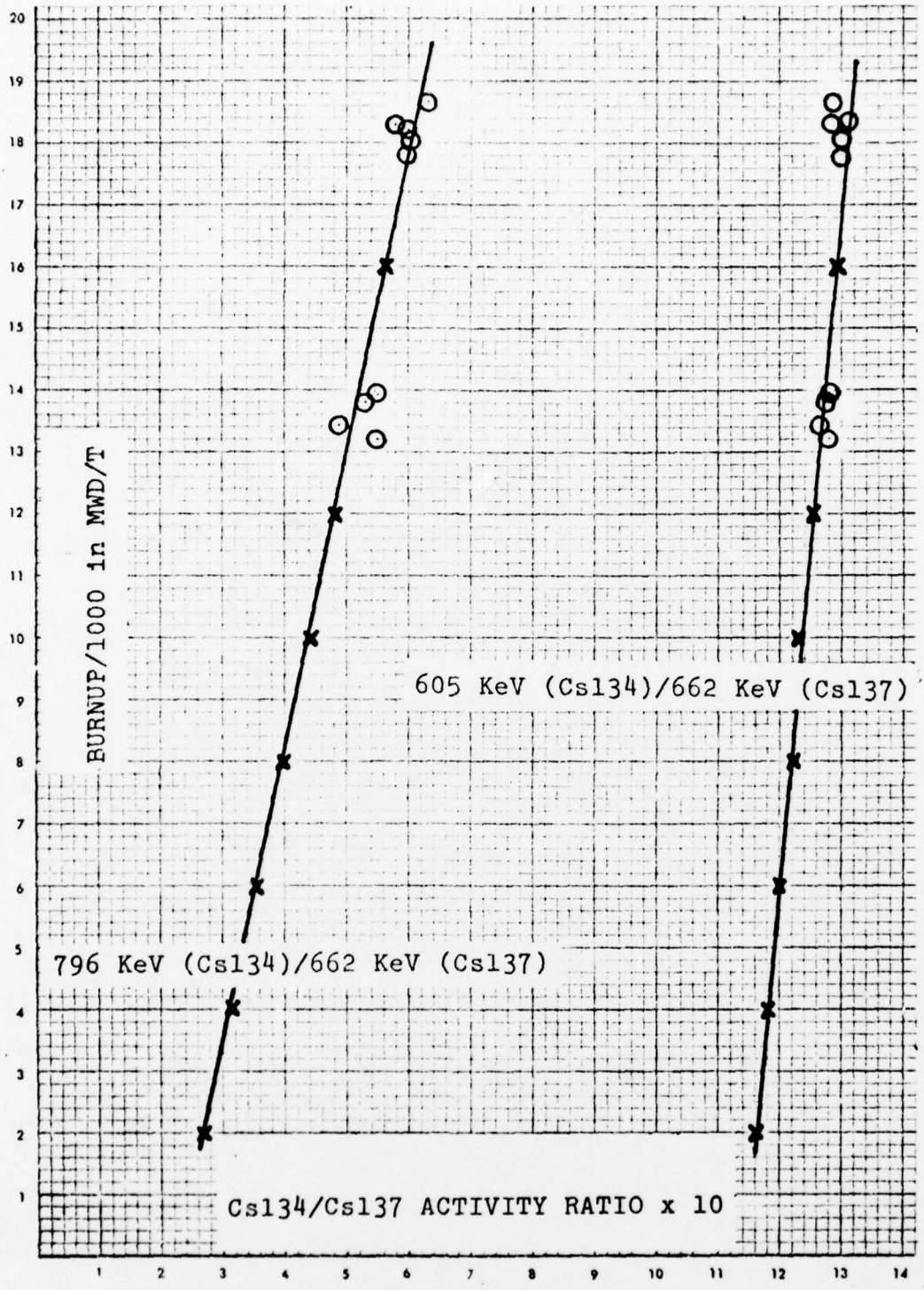

Fig. 3. Burnup Versus Cs134/Cs137 Activity Ratio at 0.42 Years Cooling Time for Different Gamma Lines of Cs134

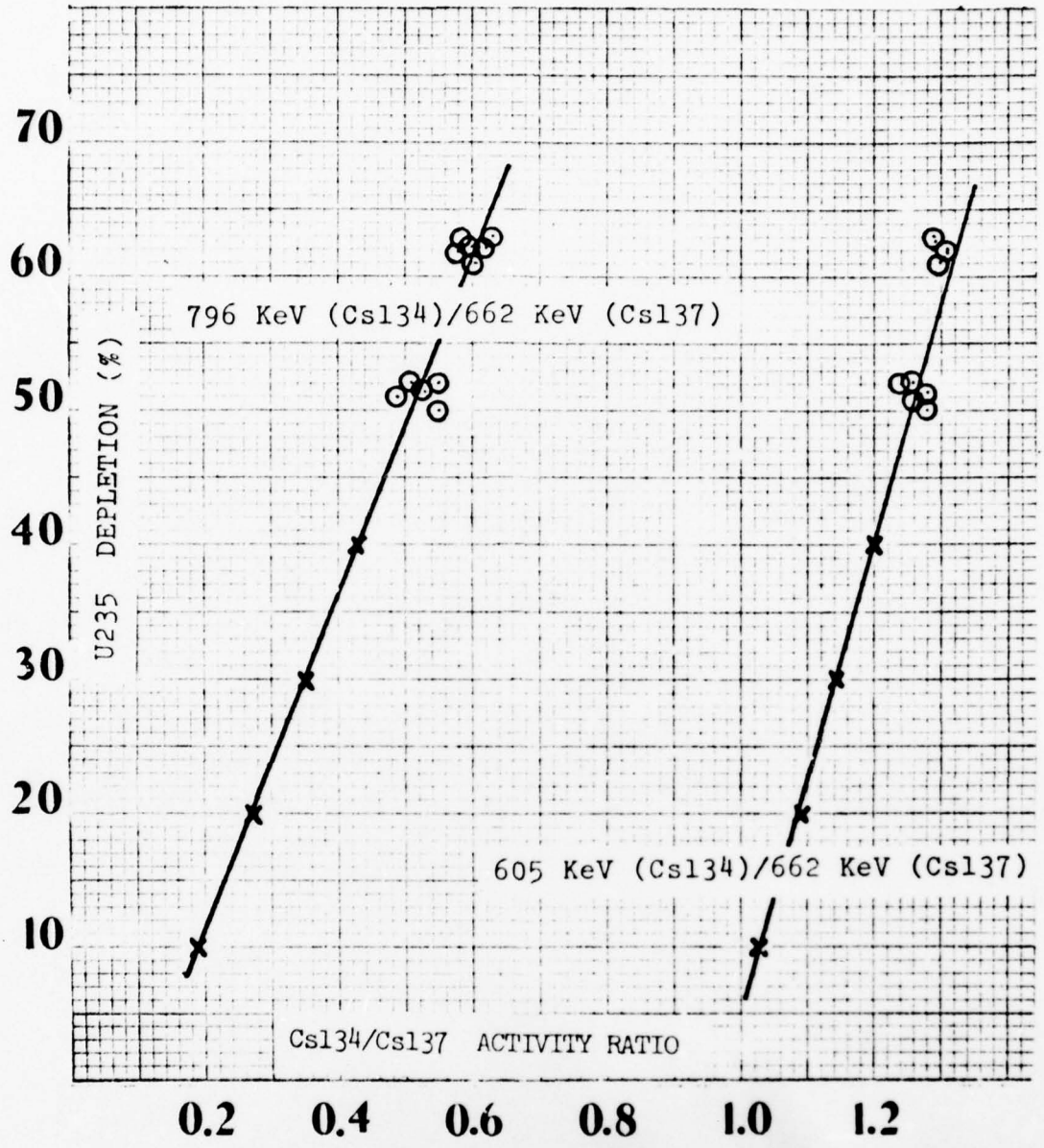

Fig. 4. U235 depletion versus Cs134/Cs137 activity ratio at 0.42 years cooling time for different gamma lines of Cs134

lating the Cs134/Cs137 activity ratio to the ratio Pu/U in irradiated fuel assemblies (Ref 23); fortunately, their results are presented in a manner which permits the Cs134/Cs137 activity ratio to be correlated to burnup. They measure the gamma spectrum of twelve fuel assemblies in the spent fuel pond of the Trino PWR reactor; cooling time is not reported. The burnup values are generated by a two-dimensional burnup code (BURSQUID) using three neutron energy groups (2 thermal, 1 fast); previous experiments validate the accuracy of the code. While Dragnev and Beets measure each assembly at only a single point, Bresesti and Peroni measure each corner of the assembly at nine levels. The countings for the nine points are summed, and then the areas of the photopeaks for the four corners are summed to give an integral value for the entire fuel assembly. This integral spectrum for the fuel assembly corresponds to a total counting time of 96 minutes.

Three sets of activity ratios are reported: Cs134(605 KeV)/Cs137 (663KeV), Cs134 (796+802)/Cs137(662), Cs134 (1365)/CS137(662). These ratios are plotted versus burnup in Fig. 5; the circles represent data from fuel assemblies with an initial enrichment of 3.13%, and the x's represent fuel assemblies with an initial enrichment of 3.90%. The lines represent a least squares fit to the data; R values are: 0.8393 for the 605 KeV data, 0.5679 for the (796+802) KeV data, 0.6946 for the 1365 KeV data.

Bresesti and Peroni also correlate Cs137 activity to

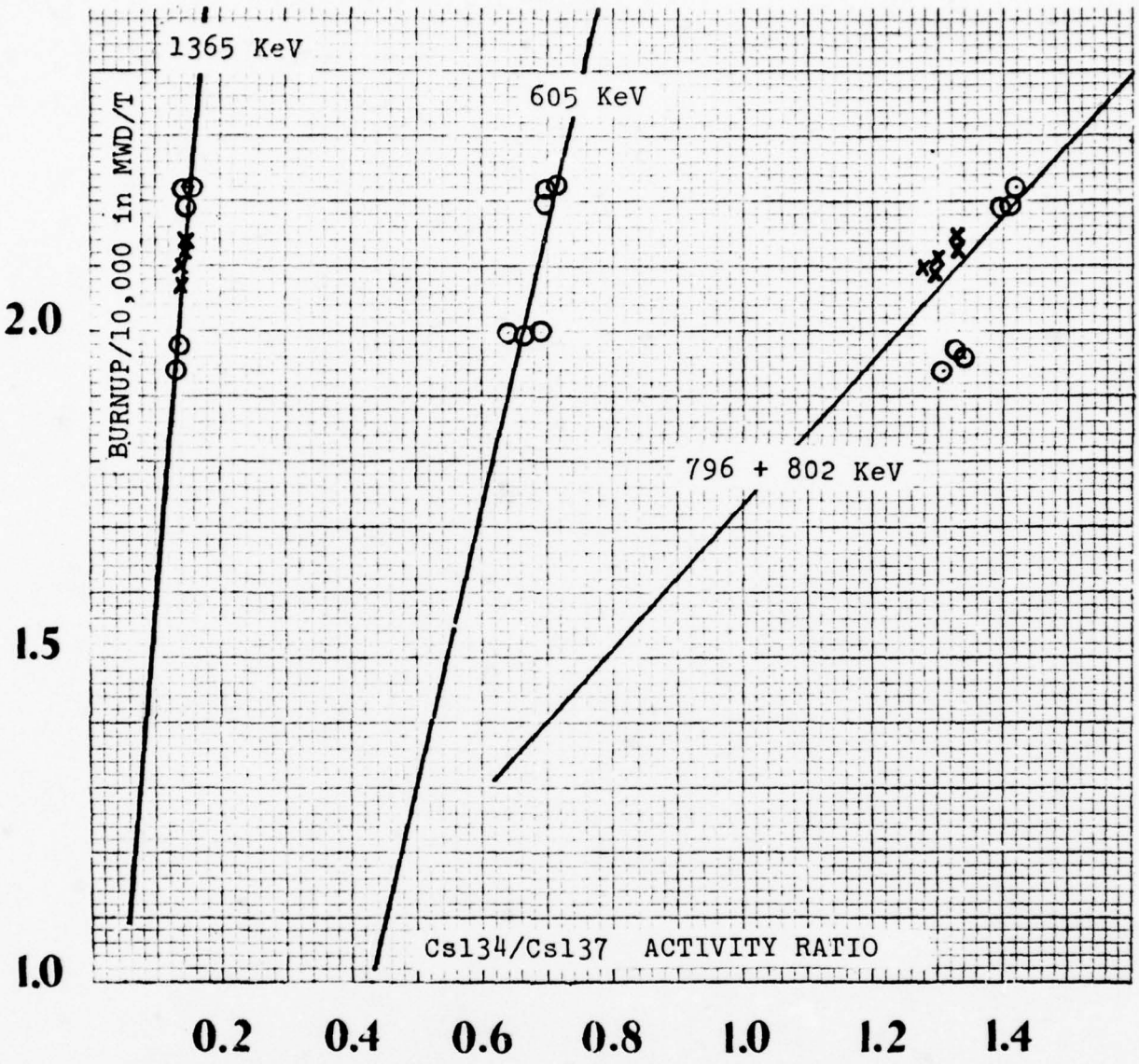

Fig. 5. Burnup Versus Cs134/Cs137 Activity Ratio for different Gamma Lines of Cs134

burnup; R is 0.865 for this correlation. This relationship is of interest because the next experiment to be examined deals with correlation of the activity ratio Cs134/Cs137 to Cs137 activity.

Leender assumes a linear relationship between burnup and Cs137 activity; his experiment examines the relationship between Cs137 activity and the activity ratio Cs134/Cs137 (Ref 24). He measures the gamma spectrum of two sets of fuel rods from the Sena reactor; one set has half the burnup of the other (actual burnups not specified). Cs134 activity is considered to be given by the mean of the 605 and 796 KeV peaks. The relationship between Cs137 activity and the Cs134/Cs137 activity ratio for fuel rods with the lesser burnup has an R of 0.9934. R for the greater burnup rods is 0.9955.

Beets, Bemelmans and Pirard examine the Cs134/Cs137 activity ratio correlation to burnup in two phases (Ref 25). The first phase involves the non-destructive gamma spectrometric measurement of fuel assemblies in the spent fuel pool, while the second phase deals with destructive measurement (fuel is decladded and dissolved). This experiment was intended to determine the effect of mutual shielding and attenuation when entire fuel assemblies are measured. In the non-destructive phase, the gamma spectrum for each fuel assembly is measured in a single point, at the middle of the active length; the time of measurement is 15 minutes. To account for attenuation and detector efficiency effects,

a correction factor F is determined for each measurement. F is given by the relation

$$F = 0.93(C_{796} + C_{802})/C_{605} \quad (3)$$

where the C's are the areas under the Cs134 peaks. A linear correction is then applied to the measured Cs137 activity (662 KeV peak) using the relation

$$A^{137}_{CALC} = F[(C_{662} - C_{605})/(C_{796} + C_{802} - C_{605})]A^{137}_{MEAS} \quad (4)$$

where A is activity, and C662 is the area under the 662 KeV peak of Cs137. The activity ratio Cs134/Cs137 refers to the measured Cs134 activity, which is determined using the 605 KeV peak, and the calculated Cs137 activity, which is defined by Eq(4). This activity ratio is correlated to the weighted burnup, where weighted burnup is defined by the expression:

$$BW = \sum_{i=1}^{n} B(W_i/W)\, e^{(t_i - t_m)} \quad (5)$$

where

BW = weighted burnup
n = number of months of fuel cycle
B = burnup
W_i = monthly integrated power
W = total integrated power
t_i = time of irradiation
t_m = time of measurement

The non-destructive phase of this experiment results in an R of 0.9946 for the relationship between the Cs134/Cs137 activity ratio and the weighted burnup.

The destructive phase involves chemical decladding and dissolution of the fuel with nitric acid; the gamma spectrum of the solution is then measured. The activity ratio and weighted burnup are determined in the same manner as in the non-destructive phase; R for the destructive measurement phase is 0.9894.

Gualandi presents interesting results on the correlation between the Cs134/Cs137 activity ratio and the mass ratio Pu/U (Ref 26). Unfortunately, his reported data is too incomplete to permit its application to a burnup correlation as was done with the work of Bresesti. However, reexamination of the Bresesti data (Ref 23:4) demonstrates a linear relationship between burnup and the Pu/U ratio (R=0.9992); this justifies qualitative application of Gualandi's results to the correlation between the Cs134/Cs137 activity ratio and burnup. Gualandi shows that initial fuel enrichment has only a slight influence on the Cs134/Cs137 and Pu/U correlation (Fig. 6), while power history has a strong influence (Fig. 7). He concludes that safeguards application (on-site) of the Cs134/CS137 activity ratio requires a thorough knowledge of power history. Since the absence of information about power history is the premise upon which the requirement for an off-site monitor is based, the degree of power history dependence is of fundamental

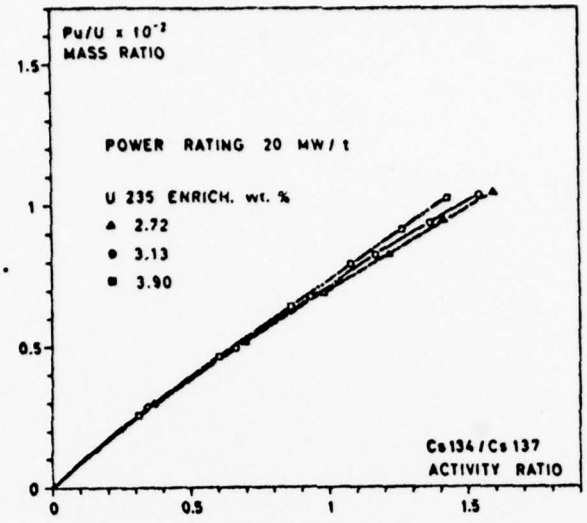

Fig. 6. Influence of the Fuel Enrichment on the Correlation Between Cs134/CS137 and Pu/U (Ref 26:618)

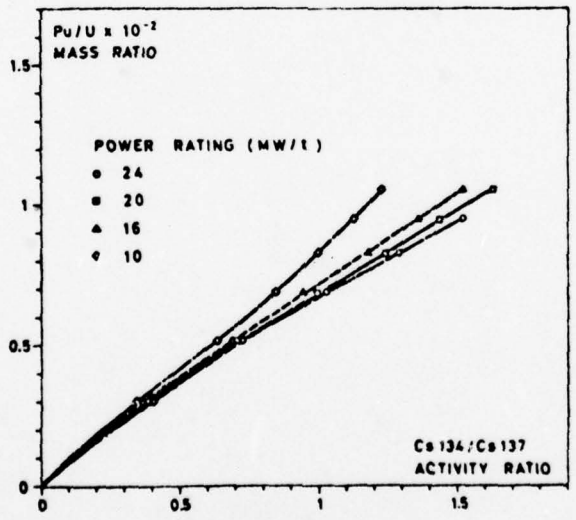

Fig. 7. Influence of the Power Rating on the Correlation between Cs134/Cs137 and Pu/U (Ref. 26:619)

importance. The power history dependence of the Cs134/Cs137 activity ratio as an indicator of burnup is analyzed in the following chapter.

Further information on the on-site application of the Cs134/Cs137 activity ratio is available in references 27 and 28; Ursu examines this ratio as an indicator of cooling time (Ref 29).

The literature survey yielded only one experiment dealing with a neodymium ratio as a burnup monitor; fortunately it examined the one ratio of interest herein, Nd146/Nd145. Before presenting an analysis of that experiment, it is necessary to define a third measure of burnup, atom percent fission. Atom percent fission (Ft) is defined as the number of fissions divided by the initial number of heavy atoms times 100(Ref 16:164). Determination of Ft burnup requires measurement of the number of atoms of a fission product monitor and the number of residual heavy atoms; the fuel specimen is dissolved and mass spectrometry used for measurement of number densities. Burnup is then calculated from the relationship:

$$F_T = 100[(M/Y)/(H+M/Y)] \qquad (6)$$

where

M = number of atoms of fission product monitor

Y = fractional fission yield of M

H = number of residual heavy atoms

The most exact fission product monitor is Nd148 (Ref 22:59).

Koch examines the correlation between Ft and the mass ratio Nd146/Nd145 (Ref 30); he uses Nd148 as the fission product monitor in determining Ft. Koch calculates a least-squares fit for measurements made on Trino fuel samples and reports the equation; his results are shown in Fig. 8. The circles represent data for the Trino fuel samples; the x's represent data for Sena fuel samples. The Sena fuel data is not used in the linear regression.

In summary, the linear relationship between the Cs134/Cs137 activity ratio and U235 depletion is well documented experimentally, although many measures of U235 depletion are used. Experimental validation of a linear relationship between the mass ratio Nd146/Nd145 and U235 depletion is sparse but convincing.

Gualandi (Ref 26) raises the issue of a power history dependence when examining the value of the cesium ratio as a burnup indicator; power history dependence is best defined by using fluence as a measure of burnup. For constant flux, fluence is the product of flux and time; a particular fluence can be obtained by different combinations of flux and time. Gualandi contends that the Cs134/Cs137 activity ratio is a function of flux and time rather than an independent function of fluence. The degree of this power history dependence is critical to the utility of the cesium ratio as an off-site indicator of burnup.

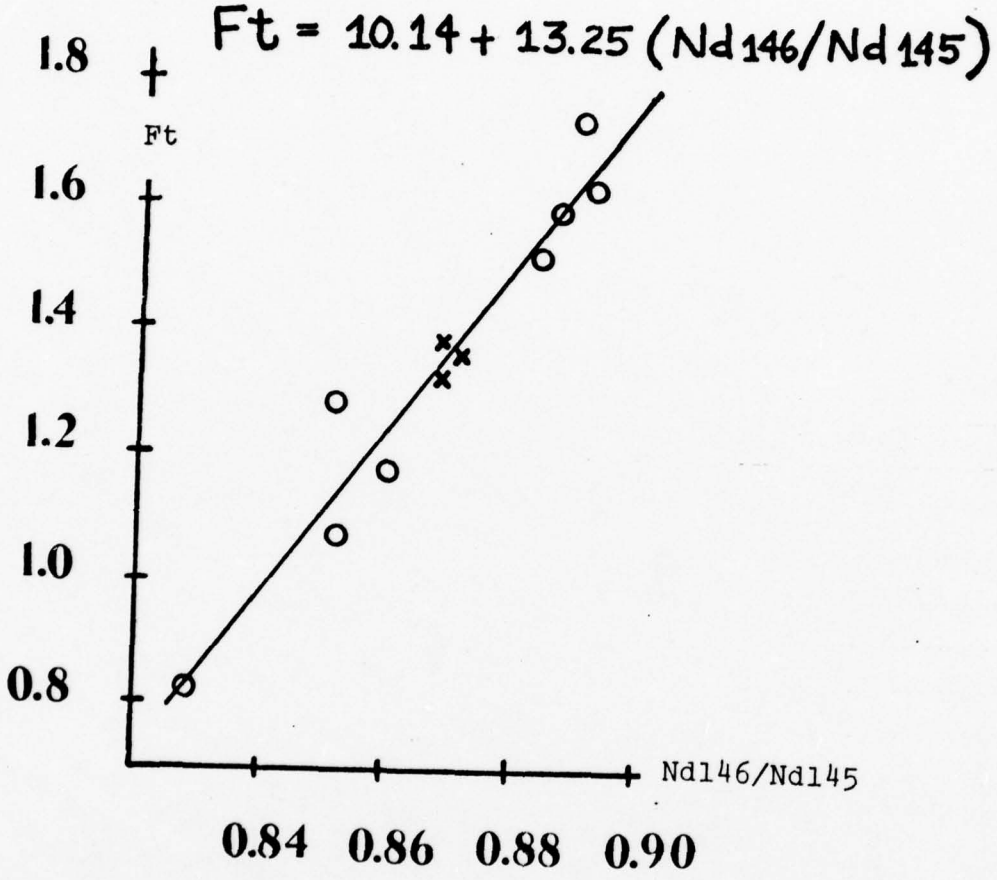

Fig. 8. Burnup versus Nd146/Nd145

IV. Power History Dependence of the Activity Ratio Cs134/Cs137 as an Indicator of Burnup

Determination of the degree of power history dependence of the activity ratio Cs134/Cs137 as an indicator of burnup requires a computer code which can calculate the accumulation and decay of fission products for varying power histories. The accumulation and decay of fission products in fuel elements can be described by a set of linear differential equations of the form (Ref 18:19):

$$dN_j^i/dt = \sum_f N_\ell^k \sigma_f \gamma_j^i \phi + N_{j-1}^i \sigma_c \phi + \lambda N_j^{i-1} - N_j^i \sigma_c \phi - \lambda N_j^i \qquad (7)$$

where

N_j^i = number of atoms of isotope of atomic number i and mass j

$\sum_f$ = sum over all fissile isotopes present in fuel

N_ℓ^k = number of atoms of fissile isotope of atomic number k and mass l

σ_f = fission cross section (barns)

γ_j^i = direct fission yield of fission product (i,j)

ϕ = neutron flux ($cm^{-2}sec^{-1}$)

σ_c = thermal capture cross section (barns)

λ = decay constant (sec^{-1})

For each fission product isotope a separate differential equation exists and these equations are coupled via N_{j-1}^i and

N_j^{i-1}; these differential equations can be solved analytically by Laplace Transform for a time constant ϕ.

Several assumptions are required to develop a simple fission product inventory code; the first of these assumptions is that the neutron flux is time constant. Actually, the irradiation history in a reactor consists of a series of constant power cycles with the neutron flux varying as a function of the fissile inventory. The second necessary assumption is that U235 is the only fissile isotope in the fuel; this assumption disregards fast fission of U238 and also the fission of accumulating plutonium.

Fig. 9 shows the production scheme for Cs134(Ref 31). Tables I and II show the nuclear data required; Table III defines the symbols used in the two preceding tables (Ref 2:65,72,79).

The final assumption is that capture cross sections less than one barn can be disregarded; the validity of this assumption will be examined when the code is completed. The largest capture cross section in the mass 132 chain (Fig. 9) is that of Xe132; since this cross section is less than 1 barn, only the mass 133 chain is required in the production scheme of Cs134. The coupled equations which must be solved are

$$dN_{133}^{Sb}/dt = N_{235}^{U}\sigma_f \gamma_{133}^{Sb}\phi + N_{132}^{Sb}\sigma_c\phi + \lambda N_{133}^{Sn}$$

$$-N_{133}^{Sb}\sigma_c\phi - \lambda N_{133}^{Sb} \qquad (8)$$

Fig. 9. Production Scheme for Cs134

TABLE I

Nuclear Data for Fissile/Isotopes (Ref. 2:72)

NUCL	DLAM	FB1	FP	FP1	FT	FA	FSF	P+6	SIGNG	FNG21	SIGF	SIGN2N	SIGN3N	Q	PG
PA234	2.85E-05	0.0	0.0	0.0	0.0	0.0		0.0	0.0	0.0	0.0	0.0	0.0	1.533	0.79
U232	3.05E-10	0.0	0.0	0.0	0.0	1.000		0.0	1.43E 02	0.0	1.55E 02	5.20E-03	6.00E-05	5.414	0.0
U233	1.36E-13	0.0	0.0	0.0	0.0	1.000		0.0	7.99E 01	0.0	5.80E 02	6.60E-03	1.26E-05	4.910	0.00
U234	8.89E-14	0.0	0.0	0.0	0.0	1.000		0.0	2.81E 02	0.0	3.86E 00	1.44E-02	8.80E-05	4.856	0.0
U235	3.09E-17	0.0	0.0	0.0	0.0	1.000		0.0	1.05E 02	0.0	4.09E 02	3.00E-02	9.40E-05	4.681	0.0
U236	9.19E-16	0.0	0.0	0.0	0.0	1.000		0.0	7.37E 01	0.0	3.24E 00	1.30E-02	1.44E-04	4.573	0.0
U237	1.19E-06	0.0	0.0	0.0	0.0	0.0		0.0	0.0	0.0	3.76E 00	0.0	0.0	0.112	0.07
U238	4.87E-18	0.0	0.0	0.0	0.0	1.000		0.0	8.35E 00	0.0	5.98E-01	3.00E-02	3.00E-04	4.268	0.0
U239	4.92E-04	0.0	0.0	0.0	0.0	0.0		0.0	0.0	0.0	0.0	0.0	0.0	0.400	0.0
U240	1.37E-05	1.000	0.0	0.0	0.0	0.0		0.0	0.0	0.0	0.0	0.0	0.0	0.211	0.21
NP236	8.75E-06	0.0	0.430	0.0	0.0	0.0		0.0	0.0	0.0	3.54E 00	0.0	0.0	0.476	0.0
NP237	1.03E-14	0.0	0.0	0.0	0.0	1.000		0.0	3.59E 02	0.0	2.45E 00	2.60E-03	1.90E-05	4.956	0.0
NP238	3.82E-06	0.0	0.0	0.0	0.0	0.0		0.0	0.0	0.0	1.01E 03	0.0	0.0	0.839	0.68
NP239	3.41E-06	0.0	0.0	0.0	0.0	0.0		0.0	1.76E 02	0.0	0.0	0.0	0.0	0.229	0.23
NP240M	1.58E-03	0.0	0.0	0.0	0.0	0.0		0.0	0.0	0.0	0.0	0.0	0.0	1.065	0.32
NP240	1.83E-04	0.0	0.0	0.0	0.0	0.0		0.0	0.0	0.0	0.0	0.0	0.0	0.280	0.0
PU236	7.71E-09	0.0	0.0	0.0	0.0	1.000		0.0	0.0	0.0	1.07E 02	0.0	0.0	5.870	0.0
PU238	2.47E-10	0.0	0.0	0.0	0.0	1.000		0.0	3.66E 02	0.0	1.94E 01	5.20E-03	6.00E-05	5.587	0.0
PU239	9.00E-13	0.0	0.0	0.0	0.0	1.000		0.0	4.43E 02	0.0	1.06E 03	1.00E-02	1.16E-04	5.243	0.0
PU240	3.25E-12	0.0	0.0	0.0	0.0	1.000		0.0	8.97E 02	0.0	2.46E 00	7.00E-03	7.00E-05	5.255	0.0
PU241	1.50E-09	0.0	0.0	0.0	0.0	0.000		0.0	3.94E 02	0.0	1.11E 03	1.58E-02	1.58E-04	0.007	0.0
PU242	5.80E-14	0.0	0.0	0.0	0.0	1.000		5.3	4.39E 02	0.0	2.22E-01	1.48E-02	1.48E-04	4.980	0.0
PU243	3.87E-05	0.0	0.0	0.0	0.0	0.0		0.0	0.0	0.0	2.58E 00	0.0	0.0	0.239	0.01
PU244	2.65E-16	0.0	0.0	0.0	0.0	0.999		1260.0	1.01E 00	0.0	0.0	0.0	0.0	4.680	0.0
PU245	1.82E-05	0.0	0.0	0.0	0.0	0.0		0.0	1.75E 02	0.0	0.0	0.0	0.0	0.400	0.0
AM241	5.07E-11	0.0	0.0	0.0	0.0	1.000		0.0	1.30E 03	0.162	4.18E 00	1.00E-03	1.00E-05	5.630	0.0
AM242M	1.45E-10	0.0	0.0	0.0	1.000	0.0		0.0	1.26E 03	0.0	3.80E 03	3.70E-02	3.80E-04	0.048	0.0
AM242	1.20E-05	0.0	0.180	0.0	0.0	0.0		0.0	0.0	0.0	1.83E 03	3.70E-02	3.80E-04	0.225	0.0
AM243	2.87E-12	0.0	0.0	0.0	0.0	1.000		0.0	5.66E 02	0.0	7.84E-01	0.0	0.0	6.158	0.12
AM244	4.44E-04	0.0	0.0	0.0	0.0	0.0		0.0	0.0	0.0	1.45E 03	0.0	0.0	1.256	0.57
AM245	9.30E-05	0.0	0.0	0.0	0.0	0.0		0.0	0.0	0.0	0.0	0.0	0.0	0.313	0.0
CM242	4.92E-08	0.0	0.0	0.0	0.0	1.000		0.1	1.90E 01	0.0	3.16E 00	0.0	0.0	6.217	0.0
CM243	6.86E-10	0.0	0.0	0.0	0.0	1.000		0.0	2.93E 02	0.0	9.95E 02	1.00E-02	1.00E-04	6.201	0.01
CM244	1.21E-09	0.0	0.0	0.0	0.0	1.000		1.3	2.23E 02	0.0	4.92E 00	0.0	0.0	5.902	0.0
CM245	2.66E-12	0.0	0.0	0.0	0.0	1.000		0.0	2.57E 02	0.0	1.47E 03	0.0	0.0	5.298	0.01
CM246	4.66E-12	0.0	0.0	0.0	0.0	1.000		262.0	4.11E 01	0.0	0.0	0.0	0.0	5.536	0.00
CM247	1.34E-15	0.0	0.0	0.0	0.0	1.000		0.0	2.08E 02	0.0	8.29E 02	0.0	0.0	5.300	0.0
CM248	6.24E-14	0.0	0.0	0.0	0.0	0.917		83300.0	5.89E 01	0.0	0.0	0.0	0.0	21.410	0.00
CM249	1.80E-04	0.0	0.0	0.0	0.0	0.0		0.0	1.77E 00	0.0	3.16E 01	0.0	0.0	0.300	0.0
CM250	1.26E-12	0.0	0.0	0.0	0.0	0.0		100000.0	1.26E 00	0.0	0.0	0.0	0.0	195.000	0.0
BK249	2.55E-08	0.0	0.0	0.0	0.0	0.000		0.0	1.33E 03	0.0	0.0	0.0	0.0	0.042	0.00
BK250	5.98E-05	0.0	0.0	0.0	0.0	0.0		0.0	2.21E 02	0.0	1.90E 03	0.0	0.0	1.507	0.61
CF249	6.24E-11	0.0	0.0	0.0	0.0	1.000		0.0	2.85E 02	0.0	2.04E 03	0.0	0.0	6.637	0.05
CF250	1.68E-09	0.0	0.0	0.0	0.0	0.992		793.0	5.06E 03	0.0	0.0	0.0	0.0	6.290	0.00
CF251	2.44E-11	0.0	0.0	0.0	0.0	1.000		0.0	2.33E 03	0.0	4.17E 03	0.0	0.0	6.039	0.02
CF252	8.30E-09	0.0	0.0	0.0	0.0	0.969		31000.0	2.72E 01	0.0	5.69E 01	0.0	0.0	12.260	0.0
CF253	4.50E-07	0.0	0.0	0.0	0.0	0.003		0.0	7.96E 00	0.0	8.22E 02	0.0	0.0	0.109	0.0
CF254	1.33E-07	0.0	0.0	0.0	0.0	0.003		996900.0	5.81E 02	0.0	0.0	0.0	0.0	194.400	0.0
ES253	3.87E-07	0.0	0.0	0.0	0.0	1.000		0.0	2.18E 02	0.0	0.0	0.0	0.0	6.747	0.0

TABLE II

Nuclear Data for Cesium Isotopes and their Precursors
(Ref 2:79)

NUCL	DLAM	FB1	FP	FP1	FT	SIGNG	FNG1	Y23	Y25	Y02	Y28	Y49	Q	FG
SN131	3.40E-03	0.0	0.0	0.0	0.0	0.0	0.0	2.90E 00	2.93E 00	1.20E 00	1.92E 00	3.78E 00	2.000	0.0
SB131	5.02E-04	0.150	0.0	0.0	0.0	0.0	0.500	0.0	0.0	0.0	1.11E 00	0.0	1.599	0.433
TE131M	6.42E-06	0.0	0.0	0.0	0.180	0.0	0.0	0.0	0.0	0.0	0.0	0.0	2.394	0.867
TE131	4.62E-04	0.0	0.0	0.0	0.0	0.0	0.0	0.0	0.0	0.0	2.02E-01	0.0	1.277	0.325
I131	9.97E-07	0.008	0.0	0.0	0.0	3.11E 00	0.0	0.0	0.0	0.0	0.0	0.0	0.589	0.678
XE131M	6.80E-07	0.0	0.0	0.0	1.000	0.0	0.0	0.0	0.0	0.0	0.0	0.0	0.328	0.500
XE131	0.0	0.0	0.0	0.0	0.0	3.40E 02	0.0	4.90E-01	0.0	4.20E-01	0.0	0.0	0.0	0.0
SN132	5.25E-03	0.0	0.0	0.0	0.0	0.0	0.0	4.30E 00	4.24E 00	2.77E 00	2.42E 00	5.10E 00	2.000	0.0
SB132M	1.54E-02	0.0	0.0	0.0	0.0	0.0	0.0	0.0	0.0	0.0	0.0	0.0	3.360	0.0
SB132	5.50E-03	0.0	0.0	0.0	0.0	0.0	0.0	0.0	0.0	0.0	1.62E 00	0.0	3.360	0.0
TE132	2.47E-06	0.0	0.0	0.0	0.0	0.0	0.500	0.0	0.0	0.0	4.04E-01	0.0	0.383	0.627
I132	8.37E-05	0.0	0.0	0.0	0.0	0.0	0.0	1.40E-01	1.40E-01	1.00E-01	3.03E-01	1.60E-01	2.907	0.817
XE132	0.0	0.0	0.0	0.0	0.0	9.46E-01	0.080	0.0	0.0	0.0	0.0	0.0	0.0	0.0
SB133	2.75E-03	0.720	0.0	0.0	0.0	0.0	0.0	3.38E 00	3.87E 00	2.46E 00	4.54E 00	4.04E 00	2.760	0.0
TE133M	2.31E-04	0.0	0.0	0.0	0.130	0.0	0.0	1.96E 00	2.24E 00	1.42E 00	0.0	2.34E 00	3.038	0.698
TE133	9.24E-04	0.0	0.0	0.0	0.0	0.0	0.0	0.0	0.0	0.0	1.01E 00	0.0	2.736	0.775
I133	9.17E-06	0.028	0.0	0.0	0.0	0.0	0.0	4.40E-01	5.00E-01	3.20E-01	0.0	1.53E-01	1.177	0.580
XE133M	3.55E-06	0.0	0.0	0.0	1.000	0.0	0.0	0.0	0.0	0.0	0.0	0.0	0.466	0.500
XE133	1.52E-06	0.0	0.0	0.0	0.0	1.51E 02	0.0	0.0	0.0	0.0	0.0	0.0	0.264	0.310
CS133	0.0	0.0	0.0	0.0	0.0	1.73E 02	0.085	0.0	0.0	0.0	0.0	0.0	0.0	0.0
SB134	4.62E-01	0.0	0.0	0.0	0.0	0.0	0.0	5.09E 00	6.90E 00	4.60E 00	3.74E 00	5.39E 00	3.878	0.052
TE134	2.75E-04	0.0	0.0	0.0	0.0	6.32E-02	0.0	0.0	0.0	0.0	2.42E 00	0.0	2.800	0.0
I134	2.19E-04	0.0	0.0	0.0	0.0	0.0	0.0	6.60E-01	9.00E-01	6.00E-01	5.05E-01	8.30E-01	3.141	0.807
XE134	0.0	0.0	0.0	0.0	0.0	7.27E-01	0.960	1.90E-01	2.60E-01	1.70E-01	0.0	2.40E-01	0.0	0.0
CS134M	6.64E-05	0.0	0.0	0.0	0.990	1.64E 00	0.500	0.0	0.0	0.0	0.0	0.0	0.291	0.526
CS134	1.07E-08	0.0	0.0	0.0	0.0	1.07E 02	0.500	0.0	0.0	0.0	0.0	0.0	1.787	0.891
BA134	0.0	0.0	0.0	0.0	0.0	6.32E-01	0.160	0.0	0.0	0.0	0.0	0.0	0.0	0.0
TE135	2.39E-02	0.0	0.0	0.0	0.0	0.0	0.0	5.05E 00	6.09E 00	4.50E 00	3.10E 00	5.70E 00	2.630	0.0
I135	2.87E-05	0.300	0.0	0.0	0.0	0.0	0.0	0.0	0.0	0.0	1.41E 00	0.0	2.112	0.827
XE135M	7.41E-04	0.0	0.0	0.0	1.000	0.0	0.0	0.0	0.0	0.0	0.0	0.0	0.527	1.000
XE135	2.09E-05	0.0	0.0	0.0	0.0	2.28E 06	0.0	1.11E 00	3.20E-01	1.00E 00	1.01E-01	1.47E 00	0.567	0.460
CS135M	2.18E-04	0.0	0.0	0.0	1.000	0.0	0.0	0.0	0.0	0.0	0.0	0.0	1.621	1.000
CS135	7.32E-15	0.0	0.0	0.0	0.0	3.23E 01	0.0	0.0	0.0	0.0	0.0	0.0	0.082	0.0
BA135M	6.71E-06	0.0	0.0	0.0	1.000	0.0	0.0	0.0	0.0	0.0	0.0	0.0	0.054	1.000
BA135	0.0	0.0	0.0	0.0	0.0	3.16E 00	0.0	0.0	0.0	0.0	0.0	0.0	0.0	0.0
I136	8.35E-03	0.0	0.0	0.0	0.0	0.0	0.0	1.80E 00	3.10E 00	2.71E 00	0.0	2.10E 00	4.527	0.589
XE136	0.0	0.0	0.0	0.0	0.0	1.78E-01	0.0	4.83E 00	3.36E 00	2.94E 00	5.96E 00	4.53E 00	0.0	0.0
CS136	6.17E-07	0.0	0.0	0.0	0.0	0.0	0.0	1.20E-01	6.80E-03	1.00E-01	3.33E-02	1.10E-01	2.317	0.932
BA136	0.0	0.0	0.0	0.0	0.0	8.58E 00	0.050	0.0	0.0	0.0	0.0	0.0	0.0	0.0
I137	3.01E-02	0.0	0.0	0.0	0.0	0.0	0.0	6.42E 00	6.00E 00	6.14E 00	0.0	6.47E 00	0.176	0.0
XE137	2.96E-03	0.0	0.0	0.0	0.0	0.0	0.0	0.0	0.0	0.0	6.26E 00	0.0	2.057	0.188
CS137	7.32E-10	0.935	0.0	0.0	0.0	1.69E-01	0.0	1.60E-01	1.50E-01	1.50E-01	1.01E-01	1.60E-01	0.276	0.011
BA137M	4.53E-03	0.0	0.0	0.0	1.000	0.0	0.0	0.0	0.0	0.0	0.0	0.0	0.663	1.000
BA137	0.0	0.0	0.0	0.0	0.0	3.89E 00	0.0	0.0	0.0	0.0	0.0	0.0	0.0	0.0
I138	1.17E-01	0.0	0.0	0.0	0.0	0.0	0.0	6.31E 00	5.74E 00	6.60E 00	0.0	6.31E 00	4.919	0.305
XE138	6.80E-04	0.0	0.0	0.0	0.0	0.0	0.0	0.0	0.0	0.0	5.56E 00	0.0	1.416	0.297
CS138	3.59E-04	0.0	0.0	0.0	0.0	0.0	0.0	0.0	0.0	0.0	5.05E-01	0.0	3.227	0.652
BA138	0.0	0.0	0.0	0.0	0.0	5.54E-01	0.0	0.0	0.0	0.0	0.0	0.0	0.0	0.0
I139	3.47E-01	0.0	0.0	0.0	0.0	0.0	0.0	5.32E 00	5.40E 00	5.69E 00	0.0	4.84E 00	2.000	0.0
XE139	1.61E-02	0.0	0.0	0.0	0.0	0.0	0.0	0.0	0.0	0.0	4.85E 00	0.0	2.730	0.267

TABLE III

Symbology and Sources of Nuclear Data (Ref 2:65)

NUCL = NUCLIDE = 10000 * ATOMIC NO + 10 * MASS NO + ISOMERIC STATE (0 OR 1) DLAM = DECAY CONSTANT (1/SEC).
FB, FP, FA, FF = FRACTIONAL DECAY BY BETA, POSITRON (OR ELECTRON CAPTURE), ALPHA, INTERNAL TRANSITION. FB = 1 - FP - FA - FF
FB1, FP1, FNG1, FN2N1 = FRACTION OF BETA, POSITRON, N-GAMMA, N-2N TRANSITIONS TO EXCITED STATE OF PRODUCT NUCLIDE
SIGTH, SIGNG, SIGF, SIGNA, SIGNP = THERMAL CROSS SECTIONS (BARNS) FOR ABSORPTION, N-GAMMA, FISSION, N-ALPHA, N-PROTON.
  SIGNG = SIGTH * (1 - FNA -FNP). SIGNA = SIGTH * FNA. SIGNP = SIGTH * FNP. FNA, FNP = FRACTION THERMAL N-ALPHA, N-PROTON.
RITH, RING, RIF, RINA, RINP = RESONANCE INTEGRAL FOR ABSORPTION, N-GAMMA, FISSION, N-ALPHA, N-PROTON.
  RING = RITH * (1 - FINA - FINP). FINA = RITH * FINA. RINP = RITH * FINP. FINA, FINP = FRACTION RESONANCE N-ALPHA, N-PROTON.
SIGMEV, SIGFF, SIGN2N, SIGNAF, SIGNPF = FAST CROSS SECTIONS (BARNS) FOR ABSORPTION, FISSION, N-2N, N-ALPHA, N-PROTON.
  SIGN2N = SIGMEV * (1 - FFF - FFNP). SIGNAF = SIGMEV * FFNA. SIGNPF = SIGMEV * FFNP. FFNA, FFNP = FRACTION FAST N-ALPHA, N-P.
Y23, Y25, Y02, Y28, Y49 = FISSION YIELD (PERCENT) FROM 233-U, 235-U, 232-TH, 238-U, 239- PU.
Q = HEAT PER DISINTEGRATION. FG = FRACTION OF HEAT IN GAMMAS OF ENERGY GREATER THAN 0.2 MEV.

EFFECTIVE CROSS SECTIONS FOR A VOLUME AVERAGED THERMAL (LT 0.876 EV) FLUX ARE AS FOLLOWS.

N-GAMMA	-	SIGNG * THERM + RING * RES.	
FISSION	-	SIGF * THERM + RIF * RES + SIGFF * FAST.	THERM = 1/V CORRECTION FOR THERMAL SPECTRUM AND TEMPERATURE.
N-2N	-	SIGN2N * FAST.	RES = RATIO OF RESONANCE FLUX PER LETHARGY UNIT TO THERMAL FLUX.
N-ALPHA	-	SIGNA * THERM + RINA * RES + SIGNAF * FAST.	FAST = 1.45 * RATIO OF FAST (GT 1.0 MEV) TO THERMAL FLUX
N-PROTON	-	SIGNP * THERM + RINP * RES + SIGNPF * FAST.	

REFERENCES

HALF LIVES, DECAY SCHEMES, AND THERMAL POWER
C M LEDERER, J M HOLLANDER, AND I PERLMAN 'TABLE OF ISOTOPES - SIXTH EDITION' JOHN WILEY AND SONS, INC (1967)
B S DZHELEPOV AND L K PEKER 'DECAY SCHEMES OF RADIOACTIVE NUCLEI' PERGAMMON PRESS (1961)
D T GOLDMAN AND JAMES P ROSSER 'CHART OF THE NUCLIDES' NINTH EDITION GENERAL ELECTRIC CO (JULY 1966)
E D ARNOLD 'PROGRAM SPECTRA' APPENDIX A OF ORNL-3576 (APRIL 1964)
CROSS SECTIONS AND FLUX SPECTRA
B F PRINCE 'NEUTRON REACTION RATES IN THE HSPE SPECTRUM' ORNL-4119, PP 79-83 (JULY 1967)
B E PRINCE 'NEUTRON ENERGY SPECTRA IN HSPE AND HSEP' ORNL-4191, PP 50-58 (DEC 1967)
M D GOLDBERG ET AL 'NEUTRON CROSS SECTIONS' BNL-325, SECOND ED, SUPP NO 2 (MAY 1964 - AUG 1966) ALSO EARLIER EDITIONS
M T KERR, UNPUBLISHED EPC COMPILATION (FEB 1968)
M K DRAKE 'A COMPILATION OF RESONANCE INTEGRALS' NUCLEONICS, VOL 24, NO 8, PP 108-111 (AUG 1966)
BNWL STAFF 'INVESTIGATION OF N-2N CROSS SECTIONS' BNWC-98, PP 84-98 (JUNE 1965)
M ALTER AND C E WEBER 'PRODUCTION OF H AND HE IN METALS DURING REACTOR IRRADIATION' J NUCL MATLS, VOL 16, PP 68-73 (1965)
L L BENNETT 'RECOMMENDED FISSION PRODUCT CHAINS FOR USE IN REACTOR EVALUATION STUDIES' ORNL-TM-1658 (SEPT 1966)
FISSION PRODUCT YIELDS
M E MEEK AND B F RIDER, 'SUMMARY OF FISSION PRODUCT YIELDS FOR U-235, U-238, PU-239, AND PU-241 AT THERMAL, FISSION SPECTRUM AND 18 MEV NEUTRON ENERGIES' APED-5398-A(REV.),(OCT. 1968)
S KATCOFF ' FISSION PRODUCTYIELDS FROM NEUTRON INDUCED FISSION' NUCLEONICS, VOL 18, NO 11, (NOV 1960)
M D DUDEY ' REVIEW OF LOW-MASS ATOM PRODUCTION IN FAST REACTORS' ANL-7434,(APRIL 1968)

THERM= 0.63200 RES= 0.33300 FAST= 2.00000

NEUTRON SOURCE= 922330 922350 942410 922380 942390 NLIBR= 2

$$dN_{133}^{Te}/dt = N_{235}^{U}\sigma_f \gamma_{133}^{Te}\phi + N_{132}^{Te}\sigma_c\phi + \lambda N_{133}^{Sb} - N_{133}^{Te}\sigma_a\phi - \lambda N_{133}^{Te} \quad (9)$$

$$dN_{133}^{I}/dt = N_{235}^{U}\sigma_f \gamma_{133}^{I}\phi + N_{132}^{I}\sigma_c\phi + \lambda N_{133}^{Te} - N_{133}^{I}\sigma_c\phi - \lambda N_{133}^{I} \quad (10)$$

$$dN_{133}^{Xe}/dt = N_{235}^{U}\sigma_f \gamma_{133}^{Xe}\phi + N_{132}^{Xe}\sigma_c\phi + \lambda N_{133}^{I} - N_{133}^{Xe}\sigma_c\phi - \lambda N_{133}^{Xe} \quad (11)$$

$$dN_{133}^{Cs}/dt = N_{235}^{U}\sigma_f \gamma_{133}^{Cs}\phi + N_{132}^{Cs}\sigma_c\phi + \lambda N_{133}^{Xe} - N_{133}^{Cs}\sigma_c\phi - \lambda N_{133}^{Cs} \quad (12)$$

$$dN_{134}^{Cs}/dt = N_{235}^{U}\sigma_f \gamma_{134}^{Cs}\phi + N_{133}^{Cs}\sigma_c\phi + \lambda N_{134}^{Xe} - N_{134}^{Cs}\sigma_c\phi - \lambda N_{134}^{Cs} \quad (13)$$

$$dN_{235}^{U}/dt = -N_{235}^{U}\sigma_a\phi \quad (14)$$

where σ_a is the absorption cross section. These equations are solved in Appendix B. These tedious hand calculations can be avoided by using the MIT code MACSYMA 272; this code's solution of Eq (14) is shown in Fig. 10.

The production scheme for Cs137 is shown in Fig. 11 (Ref 31). Since the capture cross sections for the members of the mass 136 chain are all less than 1 barn, only the mass 136 chain is required in the production scheme of Cs137. In addition to Eq (14), the coupled equations which must be solved are:

$$dN_{133}^{I}/dt = N_{235}^{U}\,\sigma_f\,\gamma_{137}^{I}\,\phi + N_{136}^{I}\,\sigma_c\,\phi + \lambda N_{137}^{Te} - N_{137}^{I}\,\sigma_c\,\phi - \lambda N_{137}^{I} \qquad (15)$$

$$dN_{137}^{Xe}/dt = N_{235}^{U}\,\sigma_f\,\gamma_{137}^{Xe}\,\phi + N_{136}^{Xe}\,\sigma_c\,\phi + \lambda N_{137}^{I} - N_{137}^{Xe}\,\sigma_c\,\phi - \lambda N_{137}^{Xe} \qquad (16)$$

$$dN_{137}^{Cs}/dt = N_{235}^{U}\,\sigma_f\,\gamma_{137}^{Cs}\,\phi + N_{136}^{Cs}\,\sigma_c\,\phi + \lambda N_{137}^{Xe} - N_{137}^{Cs}\,\sigma_c\,\phi - \lambda N_{137}^{Cs} \qquad (17)$$

The solution to these equations is contained in Appendix B. The instantaneous number of Cs134 and Cs137 atoms are given by the expressions

$$N_{134}^{Cs} = C_{66}e^{-C_2 t} - C_{68}e^{-C_3 t} + C_{70}e^{-C_{10}t} + C_{72}e^{-C_{20}t} + C_{74}e^{-C_{29}t} + C_{76}e^{-C_{40}t} + C_{78}e^{-C_{64}t} \qquad (18)$$

```
(C1) 'DIFF(N235(T),T)=-SIGA235*FLUX*N235(T);
                          D
(D1)                      -- N235(T) = - FLUX SIGA235 N235(T)
                          DT

(C2) LAPLACE(D1,T,S);

LAPLAC FASL DSK MACSYM BEING LOADED
LOADING DONE

AT FASL DSK MAXOUT BEING LOADED
LOADING DONE
(D2) S LAPLACE(N235(T), T, S) - N235(0) =

                                              - FLUX SIGA235 LAPLACE(N235(T), T, S)

(C3) LINSOLVE([%],['LAPLACE(N235(T),T,S)]);

SOLVE FASL DSK MACSYM BEING LOADED
LOADING DONE
SOLUTION

                                                        N235(0)
(E3)                 LAPLACE(N235(T), T, S) = ----------------
                                                      FLUX SIGA235 + S
(D3)                                        [E3]

(C4) ILT(E3,S,T);
                                                - FLUX SIGA235 T
(D4)                     N235(T) = N235(0) %E
```

Fig. 10 MACSYMA 272 Solution of a Differential Equation

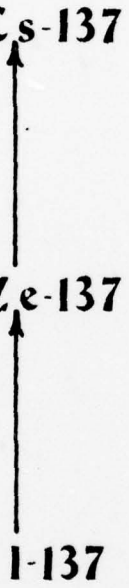

Fig. 11. Production Scheme for Cs137

$$N_{137}^{Cs} = D_{26} e^{-D_2 t} + D_{25} e^{-D_5 t} + D_{24} e^{-D_9 t} + D_{23} e^{-D_{17} t} \quad (19)$$

where the C's and D's represent constants defined in Appendix B, and t represents time.

Using these expressions for the number of Cs134 and Cs137 atoms, a cesium inventory code (TEST) was written which calculates the amount or activity of each of these isotopes with input parameters of initial amount of U235, neutron flux and time. The first application of the code was to compare it to ORIGEN (Ref 2); ORIGEN is the model used for PWR's and BWR's by the U. S. Nuclear Regulatory Commission (Ref3:28). Tables IV and V are output from ORIGEN being used to model a PWR running at a constant average specific power of 30 MW per metric ton of uranium charged to the core. The same input parameters used by ORIGEN were used in TEST; the listing and output are contained in Appendix C. The output of both programs is for 110 day increments. The depletion of U235 shown by TEST is within 1% of the depletion of U235 given by ORIGEN for the entire fuel cycle (1100 days). Fig. 12 compares the amount of Cs134 calculated by each code. TEST's result is 36% higher than ORIGEN's at 110 days; the difference decreases to 13% at 1100 days. Since all the assumptions made to

TABLE IV

Isotopic Concentrations (G-Atom/Metricton of U) of Actinides and Their Daughters as a function of Irradiation Time (Days) (Ref 2:106)

	CHARGE	110. D	220. D	330. D	440. D	550. D	660. D	770. D	880. D	990. D	1100. D
PA234	0.0	8.30E-13	1.33E-12	2.05E-12	3.03E-12	4.27E-12	5.76E-12	7.50E-12	9.49E-12	1.17E-11	1.40E-11
U232	0.0	2.50E-08	5.53E-08	9.74E-08	1.50E-07	2.42E-07	3.58E-07	5.09E-07	7.02E-07	9.38E-07	1.27E-06
U233	0.0	6.36E-06	1.12E-05	1.49E-05	1.76E-05	1.95E-05	2.07E-05	2.14E-05	2.15E-05	2.12E-05	2.06E-05
U234	1.13E 00	1.05E 00	9.84E-01	9.17E-01	8.53E-01	7.91E-01	7.31E-01	6.74E-01	6.20E-01	5.68E-01	5.19E-01
U235	1.40E 02	1.24E 02	1.09E 02	9.61E 01	8.42E 01	7.35E 01	6.38E 01	5.50E 01	4.71E 01	4.01E 01	3.40E 01
U236	0.0	3.37E 00	6.29E 00	8.84E 00	1.11E 01	1.31E 01	1.48E 01	1.62E 01	1.75E 01	1.85E 01	1.93E 01
U237	0.0	8.04E-03	1.27E-02	1.72E-02	2.15E-02	2.57E-02	2.98E-02	3.38E-02	3.77E-02	4.13E-02	4.47E-02
U238	4.06E 03	4.05E 03	4.04E 03	4.04E 03	4.03E 03	4.02E 03	4.01E 03	4.00E 03	3.99E 03	3.97E 03	3.96E 03
U239	0.0	1.78E-03	1.77E-03	1.81E-03	1.86E-03	1.92E-03	1.99E-03	2.07E-03	2.15E-03	2.24E-03	2.32E-03
U240	0.0	1.22E-34	2.06E-31	1.58E-29	3.48E-28	3.87E-27	2.80E-26	1.51E-25	6.49E-25	2.36E-24	7.51E-24
NP236	0.0	8.11E-10	1.23E-09	2.40E-09	3.94E-09	5.84E-09	8.12E-09	1.07E-08	1.37E-08	1.69E-08	2.04E-08
NP237	0.0	5.37E-02	1.60E-01	3.07E-01	4.88E-01	6.99E-01	9.32E-01	1.18E 00	1.45E 00	1.72E 00	1.99E 00
NP238	0.0	1.29E-04	3.85E-04	7.55E-04	1.24E-03	1.84E-03	2.55E-03	3.38E-03	4.30E-03	5.32E-03	6.41E-03
NP239	0.0	2.56E-01	2.55E-01	2.60E-01	2.67E-01	2.76E-01	2.86E-01	2.98E-01	3.09E-01	3.21E-01	3.33E-01
NP240M	0.0	1.05E-36	1.77E-33	1.36E-31	3.00E-30	3.34E-29	2.42E-28	1.30E-27	5.60E-27	2.04E-26	6.48E-26
NP240	0.0	6.33E-06	6.33E-06	6.57E-06	6.96E-06	7.46E-06	8.06E-06	8.72E-06	9.45E-06	1.02E-05	1.10E-05
PU236	0.0	7.89E-09	4.45E-08	1.24E-07	2.60E-07	4.62E-07	7.44E-07	1.11E-06	1.57E-06	2.13E-06	2.79E-06
PU238	0.0	1.88E-03	1.07E-02	2.99E-02	6.27E-02	1.12E-01	1.81E-01	2.71E-01	3.94E-01	5.19E-01	6.78E-01
PU239	0.0	6.73E 00	1.15E 01	1.49E 01	1.73E 01	1.89E 01	2.00E 01	2.07E 01	2.12E 01	2.15E 01	2.17E 01
PU240	0.0	3.69E-01	1.23E 00	2.34E 00	3.53E 00	4.71E 00	5.82E 00	6.82E 00	7.69E 00	8.42E 00	9.02E 00
PU241	0.0	2.61E-02	1.65E-01	4.48E-01	8.66E-01	1.39E 00	1.98E 00	2.59E 00	3.20E 00	3.77E 00	4.29E 00
PU242	0.0	6.57E-04	8.42E-03	3.55E-02	9.47E-02	1.97E-01	3.50E-01	5.56E-01	8.15E-01	1.12E 00	1.46E 00
PU243	0.0	1.92E-07	2.86E-06	1.06E-05	2.91E-05	6.28E-05	1.16E-04	1.92E-04	2.94E-04	4.20E-04	5.71E-04
PU244	0.0	6.28E-24	1.06E-20	8.14E-19	1.79E-17	2.00E-16	1.44E-15	7.76E-15	3.35E-14	1.22E-13	3.87E-13
PU245	0.0	9.03E-30	1.52E-26	1.19E-24	2.71E-23	3.13E-22	2.35E-21	1.32E-20	5.92E-20	2.25E-19	7.42E-19
AM241	0.0	9.30E-05	1.14E-03	4.51E-03	1.12E-02	2.16E-02	3.54E-02	5.17E-02	6.93E-02	8.71E-02	1.04E-01
AM242M	0.0	8.31E-07	1.76E-05	9.26E-05	2.76E-04	6.04E-04	1.08E-03	1.70E-03	2.41E-03	3.16E-03	3.89E-03
AM242	0.0	2.17E-07	2.66E-06	1.07E-05	2.75E-05	5.50E-05	9.36E-05	1.42E-04	1.99E-04	2.61E-04	3.24E-04
AM243	0.0	1.45E-05	3.73E-04	2.39E-03	8.71E-03	2.32E-02	5.07E-02	9.64E-02	1.65E-01	2.62E-01	3.88E-01
AM244	0.0	4.75E-10	1.23E-08	8.04E-08	3.01E-07	8.32E-07	1.89E-06	3.74E-06	6.69E-06	1.10E-05	1.70E-05
AM245	0.0	6.65E-28	1.06E-24	7.93E-23	1.72E-21	1.89E-20	1.36E-19	7.28E-19	3.12E-18	1.13E-17	3.56E-17
CM242	0.0	3.93E-06	9.23E-05	5.37E-04	1.76E-03	4.22E-03	8.29E-03	1.42E-02	2.19E-02	3.12E-02	4.17E-02
CM243	0.0	3.07E-09	1.43E-07	1.25E-06	5.49E-06	1.65E-05	3.92E-05	7.87E-05	1.39E-04	2.24E-04	3.32E-04
CM244	0.0	3.45E-07	1.80E-05	1.77E-04	8.86E-04	3.05E-03	8.28E-03	1.91E-02	3.89E-02	7.21E-02	1.24E-01
CM245	0.0	2.64E-09	2.66E-07	3.83E-06	2.50E-05	1.06E-04	3.38E-04	8.95E-04	2.05E-03	4.21E-03	7.89E-03
CM246	0.0	2.15E-11	4.40E-09	9.77E-08	8.78E-07	4.81E-06	1.93E-05	6.21E-05	1.70E-04	4.12E-04	9.01E-04
CM247	0.0	2.44E-14	9.97E-12	3.34E-10	4.05E-09	2.82E-08	1.38E-07	5.28E-07	1.69E-06	4.68E-06	1.16E-05
CM248	0.0	1.26E-16	1.04E-13	5.32E-12	8.82E-11	7.90E-10	4.79E-09	2.22E-08	8.40E-08	2.72E-07	7.78E-07
CM249	0.0	1.06E-21	8.73E-19	4.57E-17	7.81E-16	7.25E-15	4.58E-14	2.21E-13	8.71E-13	2.94E-12	8.75E-12
CM250	0.0	0.0	7.12E-23	5.69E-21	1.33E-19	1.58E-18	1.23E-17	7.16E-17	3.34E-16	1.31E-15	4.89E-15
BK249	0.0	1.61E-19	2.56E-16	1.92E-14	8.16E-13	4.58E-12	3.29E-11	1.76E-10	7.55E-10	2.73E-09	8.61E-09
BK250	0.0	9.23E-23	1.47E-19	1.12E-17	2.51E-16	2.87E-15	2.14E-14	1.19E-13	5.34E-13	2.01E-12	6.60E-12
CF249	0.0	3.20E-21	9.85E-18	1.06E-15	2.92E-14	3.82E-13	3.13E-12	1.85E-11	8.58E-11	3.31E-10	1.10E-09
CF250	0.0	4.09E-21	1.21E-17	1.27E-15	3.48E-14	4.56E-13	3.75E-12	2.23E-11	1.05E-10	4.09E-10	1.37E-09
CF251	0.0	3.60E-22	1.94E-18	2.85E-16	9.71E-15	1.49E-13	1.39E-12	9.13E-12	4.64E-11	1.94E-10	6.90E-10
CF252	0.0	1.51E-23	1.65E-19	3.72E-17	1.73E-15	3.42E-14	3.94E-13	3.12E-12	1.88E-11	9.11E-11	3.73E-10
CF253	0.0	0.0	9.64E-23	2.79E-20	1.54E-18	3.84E-17	4.40E-16	3.80E-15	2.47E-14	1.29E-13	5.63E-13
CF254	0.0	0.0	0.0	8.86E-24	6.29E-22	1.71E-20	2.55E-19	2.53E-18	1.85E-17	1.07E-16	5.11E-16
ES253	0.0	0.0	3.72E-23	1.40E-20	9.01E-19	2.24E-17	3.09E-16	2.83E-15	1.93E-14	1.04E-13	4.69E-13
TOTALS	4.20E 03	4.19E 03	4.17E 03	4.16E 03	4.14E 03	4.13E 03	4.11E 03	4.10E 03	4.09E 03	4.07E 03	4.06E 03
FLUX		2.58E 13	2.58E 13	2.63E 13	2.71E 13	2.81E 13	2.93E 13	3.05E 13	3.18E 13	3.31E 13	3.45E 13

TABLE V

Isotopic Concentrations/G-Atom/Metricition of U) of Fission Products as a Function of Irradiation Time (Days) Ref 2:113)

	CHARGE	110. D	220. D	330. D	440. D	550. D	660. D	770. D	880. D	990. D	1100. D
XP132	0.0	6.46E-01	1.37E 00	2.14E 00	2.95E 00	3.80E 00	4.70E 00	5.64E 00	6.63E 00	7.65E 00	8.72E 00
SB133	0.0	2.21E-05	2.20E-05	2.19E-05	2.19E-05	2.19E-05	2.20E-05	2.20E-05	2.20E-05	2.21E-05	2.21E-05
TE133M	0.0	3.35E-04	3.33E-04	3.32E-04	3.31E-04	3.31E-04	3.32E-04	3.32E-04	3.32E-04	3.33E-04	3.33E-04
TE133	0.0	3.00E-05	2.98E-05	2.97E-05	2.97E-05	2.98E-05	2.98E-05	2.99E-05	3.00E-05	3.01E-05	3.02E-05
I133	0.0	1.11E-02	1.10E-02	1.09E-02	1.09E-02	1.08E-02	1.08E-02	1.08E-02	1.08E-02	1.08E-02	1.08E-02
XE133M	0.0	6.89E-04	6.81E-04	6.77E-04	6.75E-04	6.74E-04	6.73E-04	6.73E-04	6.73E-04	6.73E-04	6.74E-04
XE133	0.0	6.67E-02	6.60E-02	6.56E-02	6.53E-02	6.51E-02	6.50E-02	6.49E-02	6.49E-02	6.48E-02	6.48E-02
CS133	0.0	8.72E-01	1.78E 00	2.65E 00	3.48E 00	4.27E 00	5.02E 00	5.71E 00	6.36E 00	6.97E 00	7.52E 00
SB134	0.0	2.26E-07	2.22E-07	2.19E-07	2.17E-07	2.16E-07	2.14E-07	2.13E-07	2.12E-07	2.11E-07	2.10E-07
TE134	0.0	3.84E-04	3.79E-04	3.74E-04	3.71E-04	3.68E-04	3.66E-04	3.65E-04	3.63E-04	3.62E-04	3.61E-04
I134	0.0	5.45E-04	5.36E-04	5.30E-04	5.26E-04	5.22E-04	5.19E-04	5.17E-04	5.15E-04	5.13E-04	5.12E-04
XE134	0.0	1.18E 00	2.34E 00	3.50E 00	4.66E 00	5.81E 00	6.95E 00	8.09E 00	9.23E 00	1.04E 01	1.15E 01
CS134M	0.0	4.99E-06	1.02E-05	1.55E-05	2.10E-05	2.67E-05	3.26E-05	3.86E-05	4.49E-05	5.12E-05	5.75E-05
CS134	0.0	1.78E-02	7.07E-02	1.55E-01	2.67E-01	4.04E-01	5.66E-01	7.50E-01	9.54E-01	1.18E 00	1.41E 00
BA134	0.0	6.30E-04	4.95E-03	1.63E-02	3.77E-02	7.19E-02	1.21E-01	1.89E-01	2.76E-01	3.84E-01	5.16E-01
TE135	0.0	3.85E-06	3.78E-06	3.74E-06	3.71E-06	3.69E-06	3.67E-06	3.65E-06	3.64E-06	3.62E-06	3.61E-06
I135	0.0	3.23E-03	3.18E-03	3.15E-03	3.12E-03	3.10E-03	3.09E-03	3.07E-03	3.06E-03	3.05E-03	3.04E-03
XE135M	0.0	3.76E-05	3.70E-05	3.67E-05	3.65E-05	3.63E-05	3.61E-05	3.60E-05	3.59E-05	3.58E-05	3.58E-05
XE135	0.0	1.25E-03	1.25E-03	1.24E-03	1.22E-03	1.19E-03	1.16E-03	1.13E-03	1.10E-03	1.07E-03	1.04E-03
CS135M	0.0	1.13E-07	4.47E-07	9.96E-07	1.77E-06	2.79E-06	4.06E-06	5.60E-06	7.42E-06	9.53E-06	1.19E-05
CS135	0.0	2.45E-01	4.94E-01	7.41E-01	9.85E-01	1.23E 00	1.46E 00	1.70E 00	1.93E 00	2.16E 00	2.40E 00
BA135M	0.0	2.45E-10	1.93E-09	6.47E-09	1.54E-08	3.05E-08	5.36E-08	8.67E-08	1.32E-07	1.92E-07	2.68E-07
BA135	0.0	3.32E-08	4.21E-07	2.03E-06	6.33E-06	1.55E-05	3.23E-05	6.04E-05	1.04E-04	1.70E-04	2.62E-04
I136	0.0	5.31E-06	5.09E-06	4.92E-06	4.78E-06	4.66E-06	4.55E-06	4.45E-06	4.36E-06	4.27E-06	4.18E-06
XE136	0.0	1.64E 00	3.30E 00	4.97E 00	6.65E 00	8.35E 00	1.01E 01	1.18E 01	1.35E 01	1.53E 01	1.70E 01
CS136	0.0	7.35E-04	1.31E-03	1.86E-03	2.40E-03	2.95E-03	3.51E-03	4.11E-03	4.73E-03	5.39E-03	6.05E-03
BA136	0.0	2.35E-03	8.42E-03	1.78E-02	3.04E-02	4.62E-02	6.54E-02	8.80E-02	1.14E-01	1.44E-01	1.78E-01
I137	0.0	3.00E-06	2.98E-06	2.98E-06	2.98E-06	2.99E-06	2.99E-06	2.99E-06	3.00E-06	3.00E-06	3.01E-06
XE137	0.0	3.18E-05	3.17E-05	3.17E-05	3.18E-05	3.18E-05	3.19E-05	3.20E-05	3.21E-05	3.23E-05	3.24E-05
CS137	0.0	9.09E-01	1.82E 00	2.73E 00	3.64E 00	4.55E 00	5.45E 00	6.35E 00	7.25E 00	8.15E 00	9.04E 00
BA137M	0.0	1.37E-07	2.75E-07	4.13E-07	5.50E-07	6.87E-07	8.24E-07	9.60E-07	1.10E-06	1.23E-06	1.37E-06
BA137	0.0	3.16E-03	1.27E-02	2.85E-02	5.07E-02	7.92E-02	1.14E-01	1.55E-01	2.02E-01	2.56E-01	3.16E-01
I138	0.0	7.37E-07	7.36E-07	7.36E-07	7.38E-07	7.39E-07	7.41E-07	7.43E-07	7.44E-07	7.46E-07	7.48E-07
XE138	0.0	1.33E-04	1.32E-04	1.33E-04	1.33E-04	1.33E-04	1.34E-04	1.34E-04	1.35E-04	1.35E-04	1.36E-04
CS138	0.0	2.52E-04	2.51E-04	2.52E-04	2.53E-04	2.54E-04	2.55E-04	2.56E-04	2.57E-04	2.58E-04	2.59E-04
BA138	0.0	8.53E-01	1.72E 00	2.58E 00	3.46E 00	4.34E 00	5.23E 00	6.12E 00	7.01E 00	7.91E 00	8.81E 00
I139	0.0	2.29E-07	2.28E-07	2.21E-07	2.19E-07	2.16E-07	2.15E-07	2.13E-07	2.11E-07	2.10E-07	2.08E-07
XE139	0.0	5.12E-06	5.01E-06	4.95E-06	4.90E-06	4.86E-06	4.82E-06	4.79E-06	4.77E-06	4.74E-06	4.72E-06
CS139	0.0	8.13E-05	7.97E-05	7.87E-05	7.79E-05	7.72E-05	7.67E-05	7.62E-05	7.58E-05	7.55E-05	7.51E-05
BA139	0.0	7.19E-04	7.08E-04	6.95E-04	6.88E-04	6.83E-04	6.78E-04	6.74E-04	6.71E-04	6.68E-04	6.65E-04
LA139	0.0	9.55E-01	1.90E 00	2.83E 00	3.76E 00	4.67E 00	5.58E 00	6.48E 00	7.38E 00	8.26E 00	9.14E 00
XE140	0.0	1.34E-06	1.31E-06	1.29E-06	1.28E-06	1.27E-06	1.26E-06	1.25E-06	1.24E-06	1.23E-06	1.23E-06
CS140	0.0	8.73E-06	8.53E-06	8.41E-06	8.31E-06	8.23E-06	8.17E-06	8.11E-06	8.06E-06	8.01E-06	7.97E-06
BA140	0.0	1.55E-01	1.52E-01	1.50E-01	1.49E-01	1.47E-01	1.46E-01	1.45E-01	1.44E-01	1.43E-01	1.42E-01
LA140	0.0	2.03E-02	2.00E-02	1.98E-02	1.96E-02	1.95E-02	1.94E-02	1.93E-02	1.93E-02	1.93E-02	1.92E-02
CE140	0.0	7.86E-01	1.74E 00	2.68E 00	3.62E 00	4.55E 00	5.48E 00	6.41E 00	7.33E 00	8.25E 00	9.17E 00
XE141	0.0	6.08E-08	5.95E-08	5.88E-08	5.82E-08	5.78E-08	5.75E-08	5.72E-08	5.70E-08	5.68E-08	5.67E-08
CS141	0.0	2.41E-06	2.33E-06	2.27E-06	2.23E-06	2.19E-06	2.16E-06	2.13E-06	2.10E-06	2.08E-06	2.05E-06
BA141	0.0	1.48E-04	1.44E-04	1.41E-04	1.38E-04	1.36E-04	1.34E-04	1.33E-04	1.31E-04	1.30E-04	1.29E-04
LA141	0.0	1.95E-03	1.90E-03	1.86E-03	1.83E-03	1.80E-03	1.77E-03	1.75E-03	1.73E-03	1.72E-03	1.70E-03
CE141	0.0	3.54E-01	3.79E-01	3.75E-01	3.69E-01	3.64E-01	3.60E-01	3.56E-01	3.52E-01	3.48E-01	3.45E-01
PR141	0.0	5.69E-01	1.45E 00	2.33E 00	3.21E 00	4.07E 00	4.91E 00	5.74E 00	6.56E 00	7.37E 00	8.16E 00

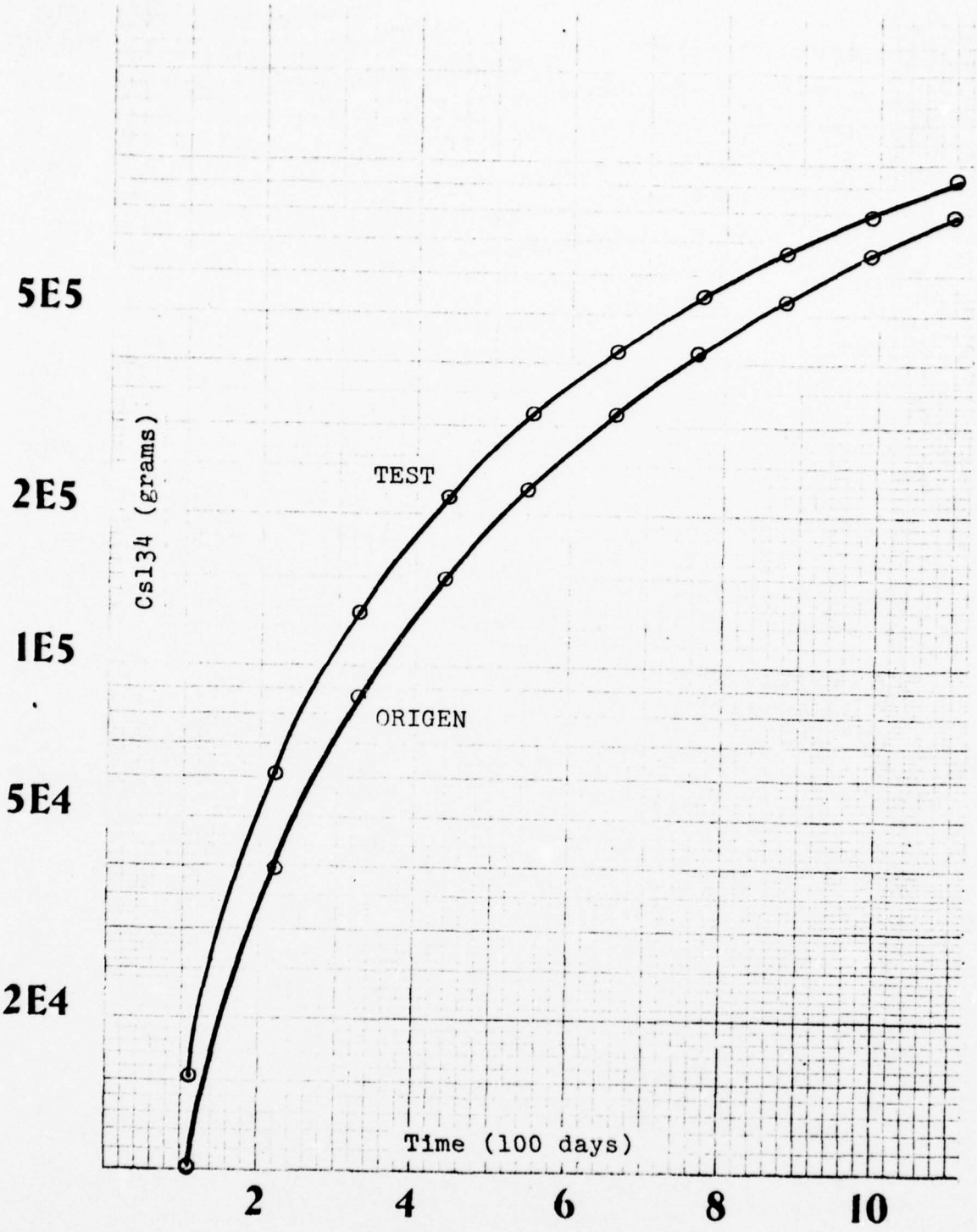

Fig. 12. Cs134 Buildup Versus Time for Codes TEST and ORIGIN

simplify TEST tend to decrease the production rate of Cs134, TEST was expected to calculate a lower value of Cs134 than ORIGEN. That TEST calculates a higher value than ORIGEN causes the accuracy of the mathematical methods used in ORIGEN to be suspect. The relative decrease in amount of Cs134 (+36% to +13%) with increasing time is as expected. ORIGEN accounts for the fission of accumulating Pu239, while TEST considers only U235 fission.

Fig. 13 compares the amount of Cs137 calculated by each code. TEST's result is 35% higher than ORIGEN's at 110 days and 4% lower at 1100 days. Again, the relative decrease in amount of Cs137 (+35% to -4%) is due to the fact that TEST disregards the fission of accumulating Pu239.

Fig. 14 compares the Cs134/Cs137 mass ratios calculated by TEST and ORIGEN; there is less than 0.1% difference at 110 days and 16% difference at 1100 days. The comparison between TEST and ORIGEN can be summarized as follows. There is close agreement on U235 depletion and Cs134/Cs137 mass ratio. TEST is 35% higher than ORIGEN for both isotopes at 110 days, but the ratio (TEST value/ ORIGEN value) decreases with time for both isotopes. It is concluded that TEST is an acceptable code for examining the power history dependence of the cesium ratio as an indicator of burnup.

The results of the comparison between TEST and ORIGEN can also be used to examine the impact of disregarding capture

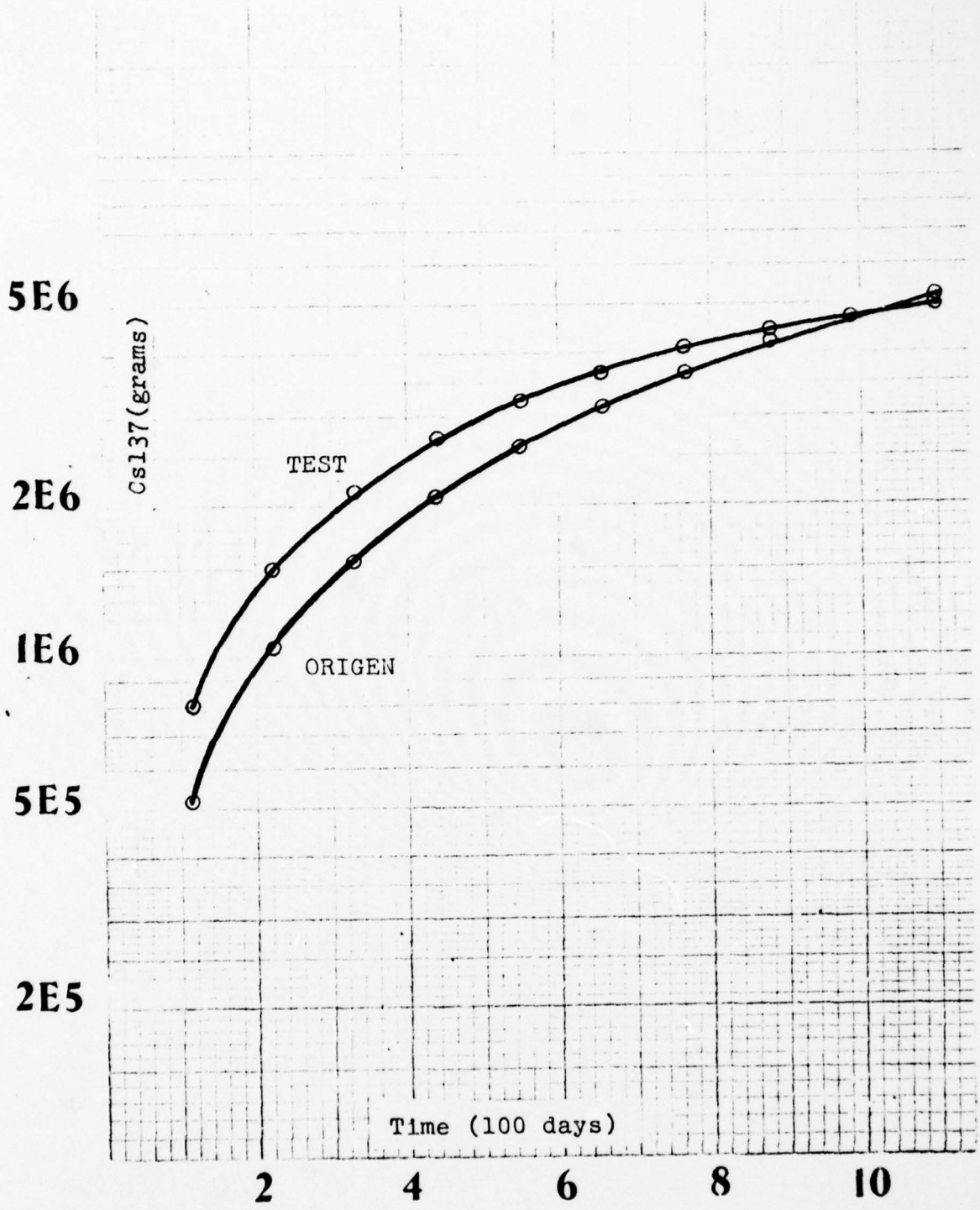

Fig. 13. Cs137 Buildup Versus Time for Codes TEST and ORIGIN

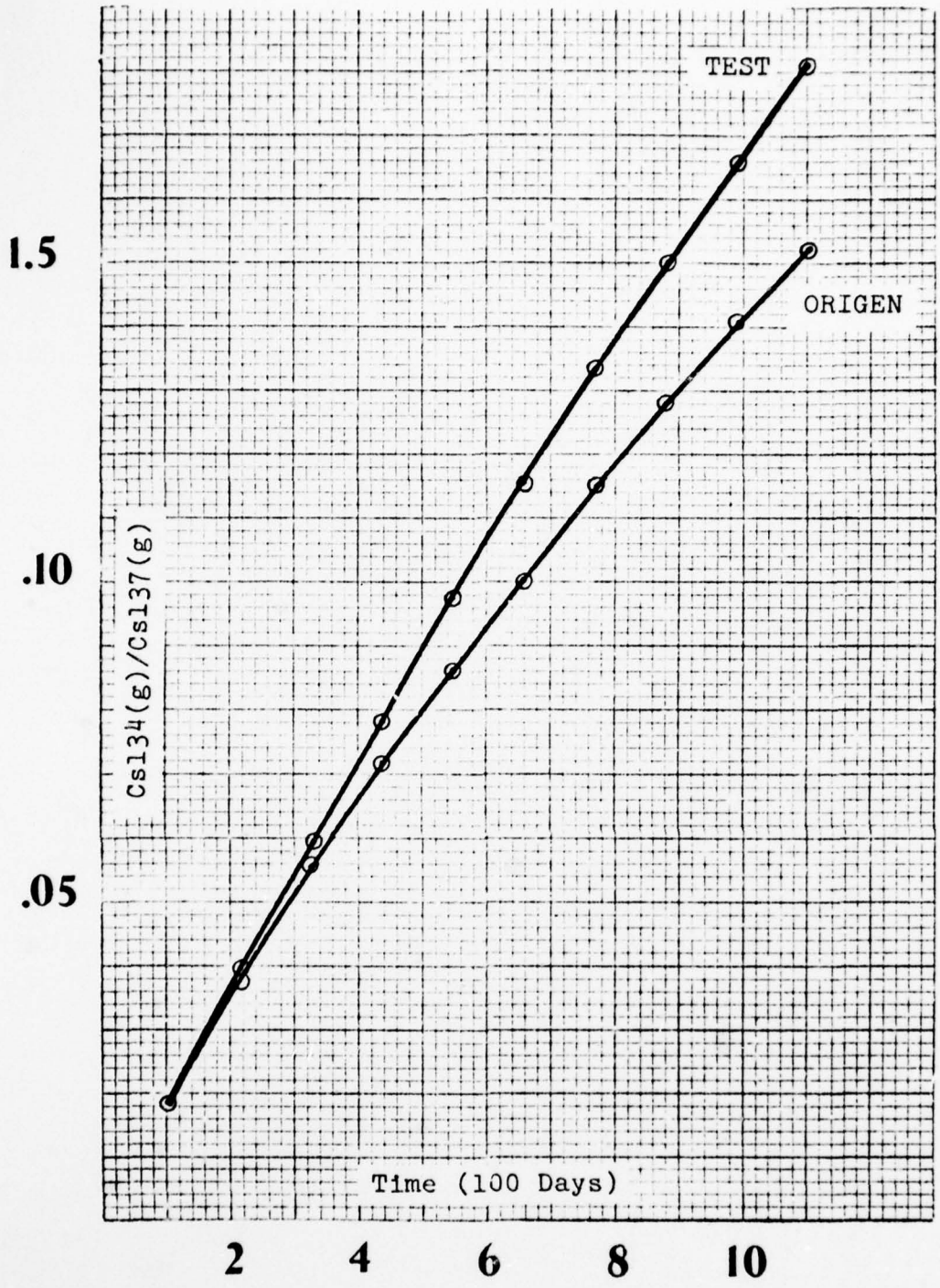

Fig. 14. Cs134/Cs137 Versus Time for Codes TEST and ORIGIN

cross sections of less than one barn in the design of the code TEST. Appendix C shows that TEST calculates 8.08E5 grams of Cs137 after 110 days and 5.00E6 grams after 1100 days. Eq (17), which is the production rate equation for Cs137, has two loss terms. One loss term is for capture, and the other is for decay. TEST disregards the capture term because the capture cross section of Cs137 is 0.169 barns. Using the above values for number of Cs137 atoms and Eq (17), loss rates due to capture and delay were calculated. At 110 days, the capture loss rate is 3.52E-6(grams/sec) and the decay rate is 5.92E-4; at 1100 days, the capture loss rate is 2.18E-5 and the decay rate is 3.66E-3. In both cases, the capture loss rate is two orders of magnitude less than the decay rate.

All applications of the code TEST hereafter described use nuclear data from Tables I and II and an initial U235 charge of 1.40E2 metric tons (same as ORIGEN PWR model). The first application of TEST to the question of power history dependence involved constant flux runs to a fluence of 8.94 E20 (neutrons per square cm). Nine flux levels (from ORIGEN PWR model operating at 30 MW per metric ton of U) were used; irradiation time required for the desired fluence was 300 days for the highest flux and 400 days for the lowest flux. Table VI lists the flux, time, and activity ratio Cs134/Cs137 for a fluence of 8.94 E20; a 25% change in flux shows only a 1.5% change in activity ratio.

TABLE VI

Activity Ratio Csl34/Csl37 (R) for Different Power Histories to a Fluence (phi x t) of 8.94 E20 (phi in neutrons per square cm sec; t in sec)

PHI=3.45E+13	T=25920000.	R=1.05638826606
PHI=3.31E+13	T=27016314.	R=1.05475135548
PHI=3.18E+13	T=28120774.	R=1.05298004049
PHI=3.05E+13	T=29319344.	R=1.05090114463
PHI=2.93E+13	T=30620136.	R=1.04866246339
PHI=2.81E+13	T=31823487.	R=1.04615216613
PHI=2.71E+13	T=32967755.	R=1.04375956784
PHI=2.63E+13	T=34001521.	R=1.04165663847
PHI=2.58E+13	T=34[illegible]0465.	R=1.0402[illegible]6422534

TABLE VII

Activity Ratio Csl34/Csl37 (R) for Different Power Histories

PHI=2.58E+13	T=2592000.	R=.05583902334553
PHI=2.63E+13	T=2592000.	R=.14336855706334
PHI=2.71E+13	T=2592000.	R=.23689057351827
PHI=1.	T=2592000.	R=.23083792016?
PHI=2.81E+13	T=2592000.	R=.33236505434247
PHI=2.93E+13	T=2592000.	R=.43183432622777
PHI=3.05E+13	T=2592000.	R=.53381323337597
PHI=3.18E+13	T=2592000.	R=.63860327430667
PHI=3.31E+13	T=2592000.	R=.74608293846877
PHI=3.45E+13	T=2592000.	R=.85646727733717
PHI=2.58E+13	T=2592000.	R=.05589902334553
PHI=2.63E+13	T=2592000.	R=.14364685706334
PHI=2.71E+13	T=2592000.	R=.23689057351827
PHI=2.81E+13	T=2592000.	R=.33308542757067
PHI=2.93E+13	T=2592000.	R=.43221406837977
PHI=3.05E+13	T=2592000.	R=.53401213038177
PHI=1.	T=2592000.	R=.52037963246937
PHI=3.18E+13	T=2592000.	R=.62989118814177
PHI=3.31E+13	T=2592000.	R=.73685794902827
PHI=3.45E+13	T=2592000.	R=.85037621604657

A second application of TEST examined more extreme variations in flux level; a listing and the output of this program are contained in Appendix D. The purpose of this program was two-fold; only the odd lines of output are addressed at this point. Ten flux levels, from 1E13 to 1E14 (neutrons per square cm sec), were run for ten time periods each; the time periods ran from 30 to 300 days, in increments of 30 days. The output lists the flux, time (sec), and activity ratio Cs134/Cs137. Recalling the theoretical correlation between fluence and Cs134/Cs137 activity ratio addressed in Chapter II, it is interesting to note that TEST shows a linear correlation coefficient of 0.9999 for this relationship for a constant flux. Returning to power history dependence, Appendix D shows that for a fluence of 2.59E20, changing the flux by a factor of 2 changes the activity ratio by 0.7%. For the same fluence, changing the flux by a factor of 5 changes the activity ratio by 12%, and a factor of 10 changes the activity by 23%. In other words, if the Cs134/Cs137 activity ratio is used as a monitor of fluence and the uncertainty in flux level is a factor of 5, then the uncertainty in fluence will be 12%.

Another way in which power history can vary is the sequence and duration of power shutdowns in fuel cycle. Table VII shows the TEST output for two power cycles with terminal fluence of 6.91E20; the flux levels are those used by the ORIGEN PWR model. Case 1 has a 30-day shutdown in the fourth month, while Case 2 has a 30-day shutdown

in the seventh month. The output lists the activity ratio at the end of each month; the difference in activity ratios at the terminal fluence is 0.7%. A similar program was run to determine the effect of shutdowns of different lengths; two fuel cycles of constant flux and 300-day duration were modeled. The first case had a flux of 7E13 with a 30-day shutdown in the fourth month; terminal fluence and activity ratio for case 1 were 1.633E21 and 1.97, respectively. Case 2 used a flux of 8E13 with a 60-day shutdown in the fourth and fifth months; terminal fluence and activity ratio were 1.659E21 and 1.99, respectively. The greater fluence (1.6%) has an activity ratio 1% higher.

The power history dependence of the Cs134/Cs137 activity ratio as an indicator of fluence can be summarized as follows. Shutdowns whose length is short compared to the half-life of Cs134 (2 yrs.) have an insignificant impact on the accuracy of the cesium ratio as an indicator of fluence. However, an order of magnitude uncertainty in the flux level of the reactor results in a 23% uncertainty in the fluence indicated by a particular cesium ratio.

As mentioned earlier, the program contained in Appendix D was designed to serve a dual purpose. The odd lines of output are for a Cs134 direct fission yield of zero, and the even lines of output are for a Cs134 direct fission yield of 5.2E-6. Goodwin cites the 5.2E-6 value (Ref 3:112); ORIGEN uses zero. The difference in amount of Cs134 calculated by TEST using these two values is

significant for low fluences; a flux of 1E13 for 30 days results in a 5% difference in Cs134 calculated. An order of magnitude increase in fluence decreases the difference in Cs134 calculated by an order of magnitude.

V. Escape from Fuel to Environment

Analysis of the escape from fuel to environment of the isotopes of interest, Csl34/137 and Ndl45/146, is addressed in three parts: escape from fuel matrix, breach of fuel cladding, escape from coolant to environment. The rate at which fission products are able to breach the cladding is determined by the burnup of the fuel; since burnup detection is the ultimate goal, breach of cladding will be examined most thoroughly.

Escape from Fuel Matrix

Fig. 15 shows the possible fission product escape mechanisms from the fuel matrix to the fuel rod plenum (Ref 32:5). The fuel matrix is a ceramic, sintered uranium dioxide; this ceramic is formed into pellets and stacked inside a Zircaloy tube. A helium-filled plenum is provided at the top of the tube (rod) to collect fission product gases. The ends of the tube are sealed with welded plugs (Ref 33:0). Prior to sealing, a helical compression spring is placed to bear on top of the pellet stack to prevent shifting of fuel pellets during handling (Ref 34:47). A temperature as high as 1800 degress C can exist in the center of a new fuel pellet operating at a linear heat generation rate of 13.4 kW/ft(Ref 35:310), while the primary coolant in a typical LWR operates at 300 degrees C.

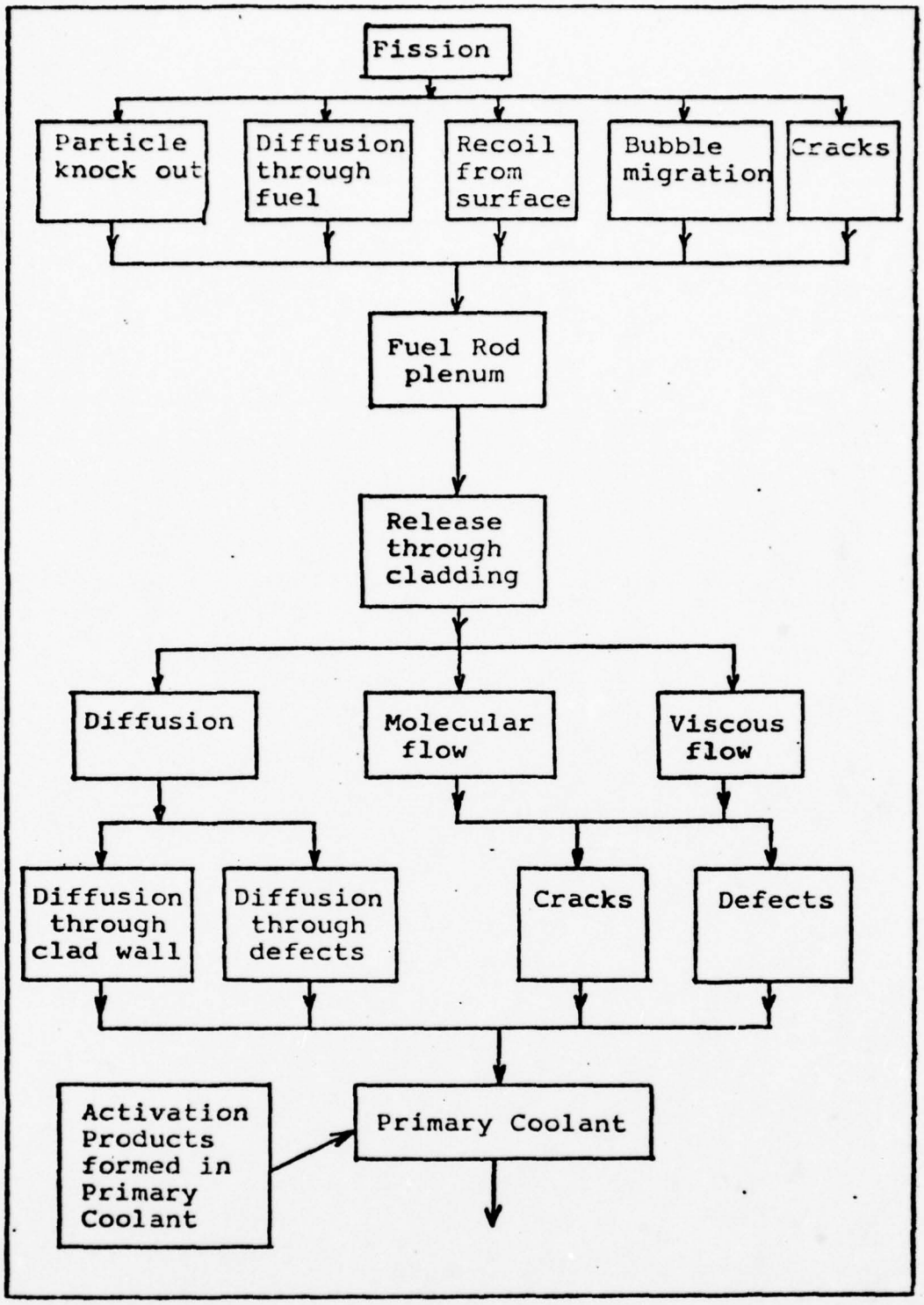

Fig. 15. Fission Product Escape Mechanisms for Fuel Matrix to Primary Coolant (Ref. 32:5)

There are four possible escape mechanisms from fuel to plenum (Ref 32:7):

(1) diffusion, trapping, and release from traps

(2) knockout release and surface effects

(3) bubble migration

(4) release through cracks in the fuel matrix

In the temperature range 800 to 1800 degrees C, fission product movement occurs by a complex diffusion trapping mechanism; the fission product atom diffuses through the fuel material until trapped. There are two categories of traps, intrinsic traps and point defects. Intrinsic traps are flaws, such as grain boundaries, in the fuel material; they are an inherent property of the material. Point defects are formed by irradiation and annealed out by heat. The trapped fission product atom is eventually released as a result of thermal agitation. This process continues until the fission product atom reaches the outside of the fuel material. The diffusion trapping mechanism is the dominant escape mode because it occurs in the temperature range where LWR fuels operate.

If a fission occurs within 20 Angstroms (A) of the surface of the fuel material, the kinetic energy of a fission fragment may drive it through the surface; some of the surface molecules are knocked out and trapped fission products released. This escape mechanism is called knockout release; below 700 degrees C, knockout release is the dominant escape mode.

Bubble migration occurs at high fuel temperatures (above 1800 degrees) when the fuel matrix begins to lose strength; bubbles form when diffusing atoms joint together. Bubble migration occurs along a thermal gradient by a mechanism called surface diffusion. The formation and movement of these bubbles causes swelling in the fuel matrix. Bubble migration is not a significant escape mode because LWR fuels do not reach a high enough temperature.

Rapid temperature changes in the fuel matrix can cause the low tensile strength ceramic to crack; diffusing fission products can then be released to the plenum by these cracks. Since rapid reactor start-up or shutdown is not a normal practice, release through cracks is not a significant escape mechanism during routine reactor operation.

Since diffusion (including trapping and release) is the dominant escape mode from fuel matrix to plenum, it is appropriate at this point to examine the diffusivity of cesium, neodymium and their precursors. Goodwin's assumption that the use of a same-element ratio ensures uniform fractional release from the fuel matrix (Ref 3:49) is not justified; the fractional release of any member of a decay chain is not simply and exclusively determined by its own diffusivity (Ref 36:89). The fact that each precursor is able to diffuse before decaying will increase the fractional release of a particular isotope above the level which estimates ignoring the mobility of precursors

would suggest. Decay products having precursors with relatively high diffusivities and half-lives which are a significant fraction of irradiation time will experience the greatest increase in fractional release.

The precursors of both neodymium isotopes of interest are cerium (Ce) and praseodymium (Pr); only Pr145 has a half-life of significant length, 6 hours (Ref 11:98). There is little to be found in the literature about the diffusivity of non-volatiles; the boiling point of neodymium and both its precursors is over 3000 degrees C. However, Brown and Faircloth state that cerium is relatively immobile (Ref 37:31), and they conclude that cerium escapes the fuel matrix only as a recoiling fission fragment. This conclusion implies that only cerium atoms produced with 10A of the surface of the fuel matrix have a chance of escaping (Ref 32:9). It is logical to assume, based on non-volatility, that Pr and Nd are as immobile as Ce. Since neither Pr nor Nd is a direct fission product (Ref 2:80), the only Nd to be found outside the fuel matrix is that formed by decaying Ce which has escaped by recoil as a fission fragment. For one of the Vak fuel pellets described in Chapter III, only 3.15E-7 of the volume lies within 10A of the surface. Even if one assumes that all cerium atoms produced in this volume recoil outward, only 3.15E-7 of the cerium atoms produced within the fuel can escape the fuel matrix. From the standpoint of escape rate, this effectively reduces the neodymium

fission yield by a factor of 3.15E-7.

The volatility of cesium gives it great mobility within the fuel matrix; it migrates radially and axially in the direction of decreasing temperature (Ref 38). Both cesium isotopes of interest have iodine and xenon as precursors, but the only half-lives of significant length in either chain are those of I133(21 hr.) and Xe133(5.27d). Since both iodine, a halogen, and xenon, a noble gas, have greater diffusivities than cesium (Ref 39), the fractional release of Cs134 should be greater than that of Cs137; Brown and Faircloth investigate and verify this experimentally (Ref 37). Friskney and Speight perform calculations to quantify this difference in fractional release (Ref 36:90); their results are shown in Fig. 16. Curves (7) and (8) apply to Cs137 because of the short half-lives of its precursors. The other curves apply to Cs134. D1 represents the diffusion coefficient of I133, and D2 refers to Xe133. D3 refers to Cs134, and the unsubscripted D refers to Cs137. Since a diffusion coefficient is a function of grain radius and temperature, two arbitrary D's are investigated, 1E-13 and 1E-14 (square cm/sec). For the worst case, D1 and D2 both an order of magnitude greater than D3, there is a difference of 27% in fractional release of the two isotopes at 100 days; this case is represented by curves (3) and (7).

The calculations of Friskney and Speight involve a simple diffusion model; it neglects both the trapping-release

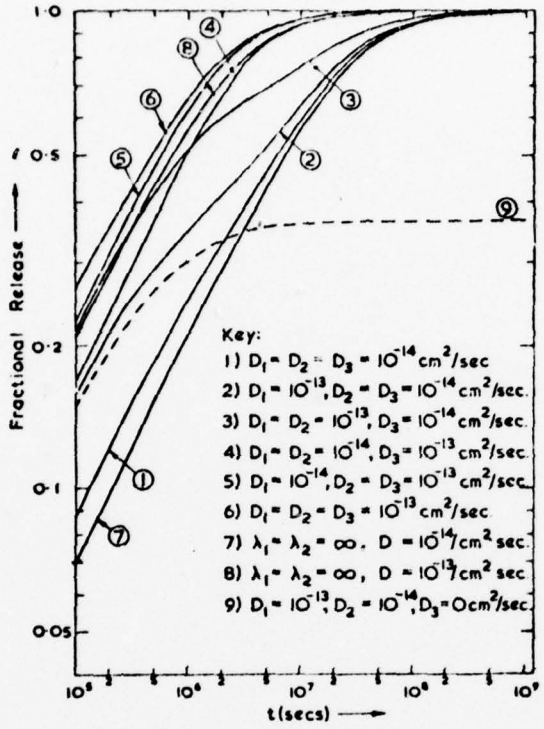

Fractional release vs time for the final stable isotope (3) in the chain:

$$1 \xrightarrow[\lambda_1]{} 2 \xrightarrow[\lambda_2]{} 3$$

(for the case of ^{133}I, ^{133}Xe, ^{133}Cs, $\lambda_1 = 9.255 \times 10^{-6}$, $\lambda_2 = 1.522 \times 10^{-6}$/sec).

Fig. 16. Fractional Release Versus Time for the Final Isotope (3) in the Chain

mechanism involved in diffusion and the fact that cesium's movement is actually a migration to lower temperature. However, their relative values of fractional release should be valid if the correct absolute diffusion coefficients are used. The unavailability of these diffusion coefficients prevents resolution of the issue of different fractional release of Cs134 and Cs137.

In summary, only a very small fraction of the neodymium (cerium) atoms can escape from the fuel matrix, while the cesium isotopes have a high, but apparently different, escape rate.

Breach of Fuel Cladding

The fuel rod cladding acts as a barrier for fission product transport and as a container for the fission gas pressure buildup; it is designed to prevent fission products from escaping to the primary coolant. Fig. 15 shows the possible escape mechanisms through the fuel cladding. Eckart calculates diffusion rate of 1.3E-4 cm/year for a noble gas in the fuel clad (Ref 32:29); the thickness of cladding on the Vak fuel described earlier is 8.5E-2 cm. It would take even the most mobile fission product 600 years to diffuse through the fuel clad; examination of the fission product content of a reactor's primary coolant demonstrates that fission product release must take place through defects in the fuel rod cladding. Stainless steel was used as fuel cladding in early LWR's, but only zirconium alloys have been used since 1968 (Ref 40).

The causes of fuel failures (clad defects) for slightly enriched uranium dioxide clad with Zircaloy are reviewed by Robertson (Ref 40); he groups the causes of fuel failure into three categories: manufacturing defects, external causes, fuel-cladding interactions.

Manufacturing defects include faulty components, faulty content and faulty assembly. Faulty components shows a very low incidence because of the simplicity of the fuel rod's design; of the 700,000 rods irradiated in 1971, none showed a fabrication defect of any kind (Ref 41:185). The most significant type of faulty content defect is contamination of the fuel by a hydrogenous compound such as water; hydrogen interacts with the Zircaloy cladding by a process called hydriding. The formation of zirconium hydride makes the clad brittle and causes a clad volume increase; these two changes in the clad can lead to cracking. The most frequent incidence of faulty assembly involved end-plug welds; but these are an insignificant contributor to fuel failure as they are usually detected by the quality control measures of the manufacturer.

External causes of clad failure include the following: fuel handling, foreign bodies, fuel overpower, vibration and fretting, cladding corrosion. In many power reactors fuel management requires that irradiated fuel assemblies be repositioned at the end of a cycle; these assemblies are then irradiated again in a subsequent cycle. This repositioning subjects the cladding to mechanical forces

when it is most susceptible to damage, i.e. when embrittled by irradiation damage and some degree of hydriding. The current design of fuel handling equipment has practically eliminated fuel handling as a cause of failure.

If a foreign body is trapped between fuel rods, it may be excited into vibration by the flow of coolant; the relatively thin cladding is then susceptible to fretting (chafing) damage. Start-up cleanliness of the primary coolant circuit precludes this failure mechanism.

Since in operation the fuel expands more than the cladding, some voidage is usually provided within the fuel rod to allow for this differential expansion. The magnitude and location of the voidage is at least roughly matched to the expected temperature distribution of the fuel, which in turn depends on the power developed in the fuel. If the power developed is considerably greater than that for which the fuel rod was designed, the cladding can be overstressed to the point of failure.

In some power reactors, vibration of the fuel assemblies has resulted in severe fretting, and even penetration of the cladding. In some instances a complete string of fuel assemblies has vibrated against a tube containing it, while in others a spacer grid or similar component has vibrated against the fuel rods.

Cladding corrosion is assigned to external causes since the corrosion resistance of Zircaloy is adequate to ensure good fuel rod performance as long as the coolant

chemistry is well controlled. Where corrosion-induced fuel failures have been reported the basic cause has been a heavy build-up of deposits on the cladding surface, resulting in the Zircaloy corrosion occuring at a much higher temperature than expected on the clad outer surface.

Fuel-cladding interactions include the following mechanisms: rod elongation, fuel densification, cladding fatigue, power ramp failures. Rod elongation and fuel densification shorten the useful life of a fuel rod, but do not actually constitute defect mechanisms; neither of these mechanisms has directly caused a reported clad rupture. Cladding fatigue also has yet to be blamed for any fuel failures in power reactors, but clad failure by fatigue was demonstrated by some early steel-clad experimental fuel rods. Power ramp failures, however, have been the direct cause of reported clad ruptures.

When reactor power is raised initially the cladding is undamaged by irradiation and fuel-cladding clearances are available to accommodate differential thermal expansion. If the power is subsequently increased from a low level to a high level, the cladding is somewhat embrittled by irradiation damage while the clearances have been at least partly taken up by fuel swelling and by the cladding creeping inward; most cladding will slowly deform under the coolant pressure by irradiation-accelerated creep. Thus there exists the potential for power ramps to crack the cladding; defect probability in ramping failures increases

with power, power increase, burnup, and dwell time at high power (Ref 42).

A fuel-cladding interaction not discussed by Robertson is fission product induced corrosion of cladding; Wood identifies iodine corrosion as a contributor to power ramp failures (Ref 42:157). Cesium has also been associated with cladding corrosion (Ref 38:144).

Of greater importance than clad failure cause is clad failure rate. Multer summarizes European fuel performance (Ref 43). For PWR's with Westinghouse stainless steel clad fuel rods and a burnup of 28,000 MWD/T, the average failure rate has been 0.02%. Zircaloy cladding has reduced the failure rate to 0.01% in some cases, but for PWR's the average failure rate remains close to 0.02%. BWR fuel has shown an average failure rate of 0.01%.

Williamson and Proebstle examine American BWR experience and recent BWR fuel improvements (Ref 44); they conclude that the newest General Electric BWR fuel is demonstrating a failure rate of 0.006%. Kramer examines the American experience with PWR fuel (Ref 45); he shows an average failure rate of 0.02% and forecasts no foreseeable improvement. The lower failure rate in BWR fuel can be attributed to the thicker cladding (.025 inch for PWR, .033 inch for BWR) and to the lower coolant pressure (2000 PSI for PWR, 1000 PSI for BWR).

In summary, breach of fuel cladding is a result of clad failure. Current clad failures are usually attributed

to hydriding and power ramps, and fission product corrosion is recognized as a contributor to power ramp failures. The current clad failure rate is 0.02% for PWR's and 0.01% for BWR's; a slight improvement in BWR fuel is forecast. Data on Combustion Engineering Inc. (C-E) and Kraftwerf Union (KWU) fuels shows similar failure rates (Ref 46).

Escape from Primary Coolant to Environment

Fig. 17 shows fission product escape mechanisms from primary coolant to environment. Environmental Protection Agency (EPA) surveillance studies describe the radwaste systems designed to prevent this escape and analyze their effectiveness (Ref 47, 48). The relative abundances of radionuclides in waste effluents are functions of (Ref 49:3):

(1) their abundance in the primary coolant

(2) their respective half-lives

(3) design of the radwaste treatment system

(4) waste treatment practices

Radwaste systems in use in American LWR's are a compromise between cost and effectiveness. The release rate of cesium by a current BWR could be reduced by a factor of 1000 with a "maximum" radwaste system costing twice as much as a current radwaste system (Ref 50:49,52); a radwaste system described by the EPA as a "minimum treatment" system would have half the cost of a current system and a cesium release rate 100 times greater. For a PWR, a "minimum treatment" radwaste system would have one-fourth the cost of a current system and a cesium release

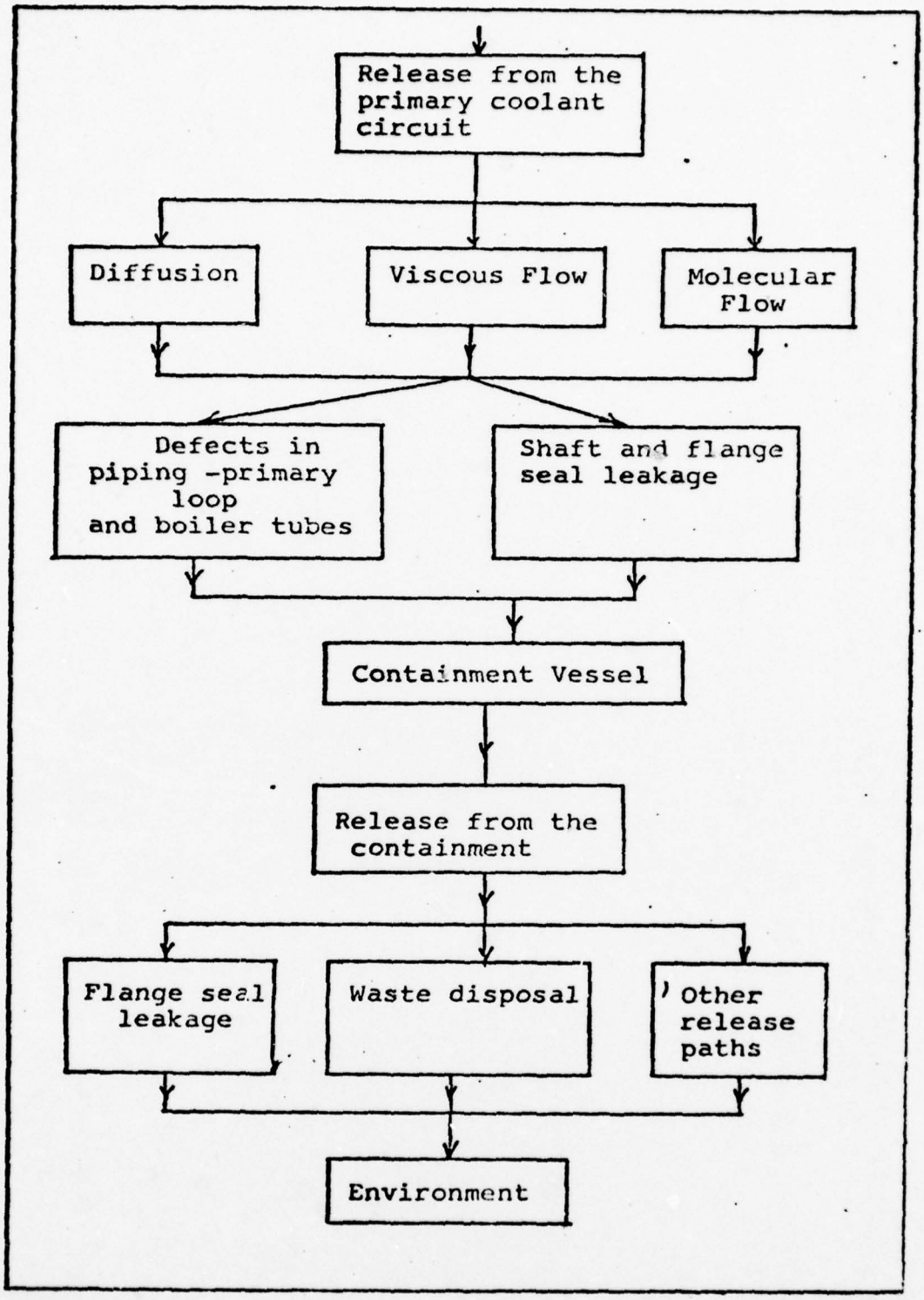

Fig. 17. Fission Product Escape Mechanisms for Primary Coolant to Environment (Ref. 32:6)

rate 100 times greater (Ref 50:59, 61).

The maximum coolant canal concentrations of Cs134 and Cs137 measured by the EPA at Dresden I, a BWR with 0.01% fuel failure rate, are 1.6E-12 Curies/L and 4.3E-12 Curies/L, respectively (Ref 10). The maximum stack release rate of Cs137 measured at Dresden is 5.5E-11 Curies/sec; no measurement is reported for Cs134. These measurements were made just before the end of a fuel cycle; some of the fuel rods were approaching maximum rated burnup.

The maximum coolant canal concentrations of Cs134 and Cs137 measured by the EPA at Haddam Neck, a PWR with 0.02% fuel failure rate, are 4.0E-13 Curies/L and 3.0E-13 Curies/L, respectively (Ref 12). The maximum stack release rates of Cs134 and Cs137 measured at Haddam Neck are 4.8E-11 Curies/sec and 3.3E-11 Curies/sec, respectively. Again, these measurements were made well into the fuel cycle when some fuel had attained high burnup.

Of the cesium concentrations reported above, the BWR has the higher reported values for both coolant canal and stack gas; the BWR values will now be used to determine the limiting distance at which the Cs134/Cs137 activity ratio could be measured.

VI. Detection

Cesium escaping through the reactor stack is a very fine particulate; particulate samples are normally collected on a filter medium with an air pump and a flow-measuring device. Gamma-spectrometric analysis for Cs134 and Cs137 requires collection of at least 1200 cubic meters of air; the minimum detectable level for both isotopes is 1E-14 Curies/cubic meter (Ref 51:10). Since the clandestine collection of such a large volume of air would require a reasonable distance between reactor and collection point, a collection point at 1500 m (1 mile) will be assumed.

Goodwin (Ref 3:70) gives a good review of various models of atmospheric dispersion; EPA uses the following generalized Guassian diffusion equation (Ref 10:97):

$$X = Q / \pi \sigma_y \sigma_z \bar{u} \, e^{-(h^2/2\sigma_z^2)} \qquad (20)$$

where

X = ground-level centerline concentration (Curies/cubic meter)

Q = release rate (Curies/sec)

σ_y, σ_z = lateral and vertical dispersion coefficients (m)

$\bar{u}$ = mean wind speed at height of release (m/sec)

h = effective release height (m)

Normalized concentrations $(X\bar{u}/Q)$ as a function of distance from the stack developed by Brookhaven are used in the

solution of this equation.

The maximum measured release rate of Cs137 at Dresden is 5.5E-11 Curies/sec. Cs134 is not reported, but can be assumed to escape with a release rate of the same order of magnitude as Cs137. The EPA reports highest ground-level centerline effluent concentrations for neutral atmospheric stability and 6 m/sec windspeed at release height (Ref 10:48); the stack height at Dresden is 91 m. Using the dispersion coefficients for these conditions, solution of Eq(20) gives a Cs137 concentration of 1.59E-16 Curies/cubic meter at 1 mile from the stack; this concentration is two orders of magnitude less than the EPA's minimum detectable level. Clearly, there are other ways to approach the detectability of a given release rate; given the atmospheric conditions, the point of maximum ground-level concentration can be calculated and assumed to be the collection point. However, the preceding calculation is so biased in favor of a high Cs137 concentration (particulate settling disregarded) that further treatment is unnecessary.

The EPA recommends a sample size of 3.5L for gamma-spectrometric analysis of cesium in water (Ref 51:10); the minimum detectable concentration is 1E-11 Curies/L. Clandestine collection of a sample of this size precludes use of the discharge canal itself; dilution by the body of water receiving the discharge canal must be assumed.

The maximum measured coolant canal concentrations at Dresden are 1.6E-12 Curies/L for Cs134 and 4.3E-12

Curies/L for Cs137. The coolant canal discharges into a river whose average flow rate is 11,000 cubic feet/sec (cfs); the dilution rate in such a situation is a function of an unmanageable number of variables. EPA, however, uses a very simplistic approach to arrive at a dilution factor of 50 (Ref 10:60). Another EPA report calculates a dilution factor of 25 for a river with average flow rate of 18,000 cfs (Ref 12:67). The lower dilution factor will be used in the interest of maximizing the cesium concentration at the collection point. Dilution of the canal concentrations by a factor of 25 results in sample concentrations of 6.4E-14 Curies/L for Cs134 and 1.72E-13 Curies/L for Cs137; these concentrations are two orders of magnitude less than EPA's minimum detectable level. Again, this calculation has been biased toward a high cesium concentration.

The fact that the EPA's minimum detectable level (MDL) for cesium in water is an order of magnitude greater than the reported coolant canal level is explained by the fact that the MDL required for measuring a cesium ratio is an order of magnitude greater than the MDL required for simple measurement of cesium. The canal levels are just above the MDL for simple measurement of cesium.

The accuracy of this type of measurement is addressed by Gans (Ref 52); he submitted identical samples containing on the order of 1E-9 Curies/L of Cs134 and Cs137 to 28 laboratories in Germany and Holland that routinely perform

analytical work for the nuclear industry. He reports a 10% variation in the measurements reported; furthermore, he predicts errors on the order of 100% when measuring concentrations close to the MDL's used herein.

VII. Results, Conclusions and Recommendations

Using measured effluent concentrations of Cs134 and Cs137 from an American BWR with a characteristic fuel failure rate of 0.01%, calculated concentrations at assumed sample collection points are two orders of magnitude less than EPA prescribed minimum detectable levels. These calculations are biased toward the high side, and the problem of different release rates of the cesium isotopes from the fuel matrix is disregarded. If minimum radwaste systems are assumed, the sample concentrations might approach minimum detectable level, but measurements at this low level of concentration are of questionable accuracy. It is concluded that the activity ratio Cs134/Cs137 is not an acceptable off-site indicator of burnup.

The neodymium isotopes, Nd145 and Nd146, have fission yields of the same order of magnitude as Cs137, but only 3.15E-7 of neodymium's precursor is able to escape the fuel matrix. Clearly, the collection point concentration of neodymium will be far less than that of cesium; conversion of the expected Cs137 concentration (using minimum radwaste system) to a number density and reduction of this number density by a factor of 3.15E-7 gives an expected neodymium number density on the order of 1 atom/L for a liquid sample and 10 atoms/L for an air sample. Measurement of such levels is not possible; the ratio Nd146/Nd145 is not acceptable as an off-site indicator of burnup.

Radioactive noble gases have been successfully measured by the EPA at 1 mile from the stack; it is recommended that radioactive isotopes of Xenon and Krypton be examined as indicators of burnup.

Bibliography

1. Weitcamp, C., et al. "The role of Nuclear Data in Nuclear Material Safeguards," Nuclear Data in Science and Technology, pp. 197-216. Vienna: IAEA, 1973.

2. Bell, M. J. Origen - The ORNL Isotope Generation and Depletion Code. Oak Ridge: Union Carbide Corporation, 1973.

3. Goodwin, R.C. "Nuclear Safeguards Implications of Off-Site Fission Product Monitoring of Commercial Power Reactors." MS thesis, AFIT/GNE/PH/78-4.

4. Foggi, C. "Isotope Correlations Based on Fission-Product Nuclides in LWR Fuels," Safeguarding Nuclear Materials, pp 425-438. Vienna: IAEA, 1976.

5. Maeck, W. J. Proposed Determination of Nuclear Fuel Burnup Based on the Ratio of Two Stable Fission Products of the Same Element. Idaho Falls, Id.: Phillips Petroleum Co., 1965.

6. Hick, H. and M. Lammer. "Interpretation of Gamma-spectrometric Measurements on Burnt Fuel Elements," Proceedings of Int. Conf. Progress in Safeguards Techniques. Vienna: IAEA, 1970.

7. Lederer, C. M. Table of Isotopes, 6th ed. New York: Wiley and Sons, 1967.

8. Weast, R. C. Handbook of Chemistry and Physics, 49th ed. Cleveland: Chemical Rubber Co., 1968.

9. RG1.21. U. S. Atomic Energy Commission Regulatory Guide. Washington: USAEC, 1974.

10. Kahn, B., et al. Radiological Surveillance Studies at a Boiling Water Nuclear Power Reactor. Cincinnati: Environmental Protection Agency, 1971.

11. Hyde, E. K., et al. Nuclear Properties of the Heavy Elements, III. Englewood Cliffs, N. J.: Prentice Hall, 1964.

12. Kahn, B., et al. Radiological Surveillance Study at the Haddam Neck PWR Nuclear Power Station. Cincinnati: USEPA, 1974.

13. Sanatani, S. and P. Siwy. "IAEA Bank of Correlated Isotopic Composition Data," Safeguarding Nuclear Materials, pp 439-448. Vienna: IAEA, 1976.

14. Foggi, C. and W. L. Zijp. "Data Treatment for the Isotopic Correlation Technique," Safeguarding Nuclear Materials, pp 405-424. Vienna: IAEA, 1976.

15. Eder, O. J. and M. Lammer. "Influence of Uncertainties in Fission Product Nuclear Data on the Interpretation of Gamma-spectrometric measurements on Burnt Fuel Elements," Nuclear Data in Science and Technology, pp 233-268. Vienna: IAEA, 1973.

16. Maeck, W. J. "Fission Product Nuclear Data Requirements for the Determination of Nuclear Fuel Burnup," Fission Product Nuclear Data, pp 163-190. Vienna: IAEA, 1974.

17. Weitkamp, C. "Importance of Fission Product Nuclear Data for Safeguards Techniques," Fission Product Nuclear Data, pp 191-212. Vienna: IAEA, 1974.

18. Hick, H., et al. The Establishment of Complete Fission Product Inventories for Irradiated Fuel Fuel Elements. D. P. Report 754. Dorchester, England: A.E.E. Winfrith, 1971.

19. Henry, A. F. Nuclear Reactor Analysis. Cambridge, Mass.: MIT Press, 1975.

20. Dragnev, T. and C. Beets. "Identification of Irradiated Fuel Elements," Joint Integral Safeguards Experiment (JEX 70), pp 12-44. Mol, Belgium: Euratom, 1971.

21. 1013059-2C. SR56 Applications Library. Dallas: Texas Instruments Inc., 1976.

22. Robin, M. "The Importance of Fission Product Nuclear Data in Burnup Determination," Fission Product Nuclear Data, pp 59-75. Vienna: IAEA, 1974.

23. Bresesti, M. and P. Peroni. "Gamma Measurements on Trino Fuel Assemblies, "Joint Safeguards Experiment Mol IV. Vienna: IAEA, 1975.

24. Leender, L. "Contribution to the Investigation of Isotopic Correlations among Non-Destructive Measurements on Fuel Rods, "Joint Safeguards Experiment Mol IV. Vienna: IAEA, 1975.

25. Beets, C., et al. "Gamma Measurements on Sena Spent Fuel Assemblies and Dissolver Solutions," Joint Safeguards Experiment Mol IV. Vienna: IAEA, 1975.

26. Paoletti Gualandi, M., et al. "Determination of Burnup and Plutonium Content in Irradiated Fuels by Gamma-spectrometry measurements of Radioactive Fission Products," Safeguarding Nuclear Materials. Vienna: IAEA, 1975.

27. Koch, L., et al. "Improvements and Experience in the Analysis of Reprocessing Samples," Safeguarding Nuclear Materials. Vienna: IAEA, 1976.

28. Hsue, T. "Passive Gamma Assay of Irradiated Fuel," LA-6849-PR. Los Alamos: LASL, 1977.

29. URSU, I., et al. "Cooling-Time Determination of the Nuclear Fuel For a VVR-S Reactor," Safeguarding Nuclear Materials. Vienna: IAEA, 1976.

30. Koch, L., et al. "Fission Gas Correlations," Joint Safeguards Experiment Mol IV. Vienna: IAEA, 1975.

31. Goldman, D. and J. Roesser. Chart of the Nuclides. Schenectady, N. Y.: Knolls Atomic Power Laboratory, 1966.

32. Eckart, L. "The Relative Environmental Hazard of Fission Products Released from Defective Fuel Rods." PHD Dissertation, Univ. Cincinnati, 1971.

33. Lish, K. Nuclear Power Plant Systems and Equipment. New York: Industrial Press Inc., 1972.

34. "Sequoyah Nuclear Station," Nuclear Engineering International. (October 1971).

35. 6BWR. General Description of a Boiling Water Reactor. San Jose, Calif.: General Electric, 1973.

36. Friskney, C. and M. Sepeight. "A calculation on the In-Pile Diffusional Release of Fission Products Forming a General Decay Chain," Journal of Nuclear Materials, 62: 89-94 (February 1976).

37. Brown, P. and R. Faircloth. "Metal Fission Product Behavior in High Temperature Reactors," Journal of Nuclear Materials, 59: 29-41(August 1975).

38. Lawrence, L., et al. "Cesium Relocation in Mixed Oxide Fuel Pins Resulting from Increased Temperature Reirradiation," Transactions of the American Nuclear Society, 23: 144-146 (1976).

39. Erdman, C. Radionuclide Production Transport and Release from Normal Operation of a LMFBR. Charlottesville: Univ. Virginia Press, 1975.

40. Robertson, J. "Nuclear Fuel Failures, Their Causes and Remedies," Proceedings of Joint Topical Meeting on Commercial Nuclear Fuel Technology Today. Toronto: American Nuclear Society, 1975.

41. Haywood, L., et al. Proceedings of the Fourth United Nations International Conference on Peaceful Uses of Atomic Energy, 8. Geneva; U.N., 1971.

42. Wood, J. "Environmentally Influenced Failure of Uranium Dioxide Ziracaloy Fuel," Transactions of the American Nuclear Society, 23: 157-158 (1976).

43. Multer, M. "European Operating Experience," Proceedings of Joint Topical Meeting on Commercial Nuclear Fuel Technology Today. Toronto: American Nuclear Society, 1975.

44. Williamson, H. and R. Proebstle. "Results with BWR Fuel Improvements," Proceedings of Joint Topical Meeting on Commercial Nuclear Fuel Technology Today. Toronto: American Nuclear Society, 1975.

45. Kramer, F. "PWR Fuel Performance - The Westinghouse View," Proceedings of Joint Topical Meeting on Commercial Nuclear Fuel Technology Today. Toronto: American Nuclear Society, 1975.

46. Smerd, P. and H. Stehle. "C-E/KWU Operating Experience with LWR Fuel," Transactions of the American Nuclear Society, 23: 256-257 (1976).

47. Kahn, B., et al. Radiological Surveillance Studies at a Pressurized Water Nuclear Power Reactor. Cincinnati: EPA, 1971.

48. Blanchard, R., et al. Radiological Surveillance Studies at the Oyster Creek BWR Generating Station. Cincinnati: EPA, 1976.

49. Logsdon, J. and R. Chissler. Radioactive Waste Discharges to the Environment from Nuclear Power Facilities. Rockville, Md.: U. S. Dept. of Health, Education and Welfare, 1970.

50. EPA-520/9-73-003-C. Environmental Analysis of the Uranium Fuel Cycle, II. Washington: EPA, 1973.

51. ORP/SID 72-2. Environmental Radioactivity Surveillance Guide. Washington: EPA, 1972.

52. Gans, I. "Experiences in Round Robin Tests with Samples of Liquid Effluents from Nuclear Power Stations in Germany," Environment International, 1:101-102 (1978).

Vita

James L. Clark Jr. was born 29 Jan 43 in Joplin, Missouri. He graduated from Lincoln-Sudbury Regional High School in Lincoln, Mass. in 1961 and from the University of Georgia in 1968. He then entered the U. S. Marine Corps as a Second Lieutenant and upon completion of training served as a rifle platoon commander in the Republic of Vietnam. Subsequent to this tour with the Third Marine Division he was assigned as security officer of the Philadelphia Naval Base. After 3 years in Philadelphia, he was transferred to Camp Lejeune, N. C. and served as a rifle company commander in the Second Marine Division. He then attended the Advanced Infantry Officer course at Ft. Benning, Ga. Upon graduation, he was assigned as commanding officer of the Marine Detachment aboard USS Constellation (CV-64).

In June of 1977, Captain Clark entered the Graduate Nuclear Effects program, Air Force Institute of Technology.

Permanent address: Lavonia, Ga.

Appendix A

Krypton and Xenon Effluent Concentrations Versus Background Concentrations

Molecular Fraction of Kr in Air:	1.0 E-6
Number Density of Air:	2.548 E19 cm-3
Number Density of Kr:	2.548 E13 cm-3
Kr84 Natural Abundance:	0.5690
Kr83 Natural Abundance:	0.1155
Kr84 Number Density:	1.45 E13 cm-3
Kr83 Number Density:	2 94 E12 cm-3

Molecular Fraction of Xe in Air:	8.0 E-8
Number Density of Xe:	2.04 E12 cm-3
Xe131 Natural Abundance:	0.2118
Xe132 Natural Abundance:	0.2689
Xe134 Natural Abundance:	0.1044
Xe136 Natural Abundance:	0.0887
Xe131 Number Density	4.32 E11 cm-3

Xe132 Number Density: 5.49 E11 cm-3

Xe134 Number Density: 2.13 E11 cm-3

Xe136 Number Density: 1.81 E11 cm-3

Maximum Observed Stack Gas Concentration of Kr85 at Oyster Creek: 3.2 E-7 μCi/cc

Maximum Observed Stack Gas Concentration of Xe133 at Oyster Creek: 1.9 E-4 μCi/cc

$$\text{Activity} = \lambda N$$

$$\lambda_{Kr85} = 2E\text{-}9 \text{ sec}^{-1}$$

$$\lambda_{Xe133} = 1.52E\text{-}6 \text{ sec}^{-1}$$

$$N = \text{Activity}/\lambda$$

$$N_{Kr85} = 5.92E6 \text{ cm}^{-3}$$

$$N_{Xe133} = 4.63E6 \text{ cm}^{-3}$$

For every 100 atoms of U_{235} thermally fissioned, following number of atoms created:

Kr83 — 0.48

Kr84 — 1.10

Kr85 — 1.50

Xe131 — 2.64

Xe132 — 4.35

Xe133 — 0.360

Xe134 — 7.60

Xe136 — 6.30

Kr83 and Kr84 can be expected to be present in stack gas in concentration on the order of 1E6 per cubic centimeter.

Xe131, 132, 133, 134, 136 can be expected to be present in stack gas in concentration on the order of 1E7 per cubic centimeter.

Appendix B

Cesium Production Equations

$$\frac{dN_{235}^{U}}{dt} = - N_{235}^{U} \sigma_a \phi$$

$$c_{1A} = - \sigma_a \phi$$

$$L\{N'\} = s L\{N\} - N(0)$$

$$L\{c_{1A} N\} = c_{1A} L\{N\}$$

$$sL\{N\} - N(0) = c_{1A} L\{N\}$$

$$sL\{N\} - c_{1A} L\{N\} = N(0)$$

$$L\{N\} = N(0)/s - c_{1A}$$

$$L\{e^{kt}\} = 1/s - k$$

$$N = N(0)\, e^{c_{1A} t}$$

$$N_{235}^{U} = N(0)_{235}^{U}\, e^{-\sigma_a \phi t}$$

By similar calculations, the following solutions were determined. The constants are defined in Appendix C.

$$N_{133}^{Sb} = C_5 e^{-C_2 t} - C_6 e^{-C_3 t}$$

$$N_{133}^{Te} = C_{13} e^{-C_{10} t} + C_{14} e^{-C_2 t} - C_{15} e^{-C_3 t}$$

$$N_{133}^{I} = C_{23} e^{-C_2 t} - C_{24} e^{-C_3 t} + C_{25} e^{-C_{10} t} + C_{26} e^{-C_{20} t}$$

$$N_{133}^{Xe} = C_{35} e^{-C_2 t} - C_{36} e^{-C_3 t} + C_{37} e^{-C_{10} t} + C_{38} e^{-C_{20} t} + C_{39} e^{-C_{29} t}$$

$$N_{133}^{Cs} = C_{47} e^{-C_2 t} - C_{48} e^{-C_3 t} + C_{49} e^{-C_{10} t} + C_{50} e^{-C_{20} t} + C_{51} e^{-C_{29} t} + C_{52} e^{-C_{40} t}$$

$$N_{134}^{Cs} = C_{66} e^{C_{67}} - C_{68} e^{C_{69}} + C_{70} e^{C_{71}} + C_{72} e^{C_{73}} + C_{74} e^{C_{75}} + C_{76} e^{C_{77}} + C_{78} e^{C_{79}}$$

$$N_{137}^{I} = D_7 e^{-D_2 t} + D_8 e^{-D_5 t}$$

$$N_{137}^{Xe} = D_{13} e^{-D_2 t} + D_{14} e^{-D_5 t} + D_{15} e^{-D_9 t}$$

$$N_{137}^{Cs} = D_{26} e^{D_{27}} + D_{25} e^{D_{28}} + D_{24} e^{D_{29}} + D_{23} e^{D_{30}}$$

Appendix C

Program Test

```
      PROGRAM TEST(INPUT,OUTPUT)
      REAL I133I,I137I
      DIMENSION INTEGR(6)
      DATA INTEGR/3*(-0),0,2*(-0)/
      CALL SYSTEMC(115,INTEGR)
      READ*,U235I,SIGF,SIGA
      READ*,SB133I,YSB133,DSB133
      READ*,TE133I,YTE133,DTE133
      READ*,I133I,YI133,DI133
      READ*,XE133I,XE133C,DXE133
      READ*,CS133I,CS133C
      READ*,CS134I,YCS134,DCS134,CS134C
      READ*,I137I,YI137,DI137
      READ*,XE137I,DXE137
      READ*,CS137I,YCS137,DCS137,CS137C
      READ*,T
      DO 101 I=1,10
      READ*,PHI
      C1A=U235I*SIGF*PHI
      C1=YSB133*C1A
      C2=SIGA*PHI
      C3=DSB133
      C4=SB133I
      C5=C1/(C3-C2)
      C6=(C1+(C2*C4)-(C3*C4))/(C3-C2)
      C7=YTE133*C1A
      C8=C3*C5
      C9=C3*C6
      C10=DTE133
      C11=C7+C3
      C12=TE133I
      C13=C11/(C2-C10)+C12-C9/(C3-C10)
      C14=C11/(C10-C2)
      C15=C9/(C10-C3)
      C16=YI133*C1A
      C17=C10*C13
      C18=C10*C14
      C19=C10*C15
      C20=DI133
      C21=C16+C18
      C22=I133I
      C23=C21/(C20-C2)
      C24=C19/(C20-C3)
      C25=C17/(C20-C10)
      C26=C22+C17/(C10-C20)-C19/(C3-C20)
      C27=XE133C*PHI
      C28=DXE133
      C29=C27+C28
      C30=C20*C23
      C31=C20*C24
      C32=C20*C25
      C33=C20*C26
      C34=XE133I
      C35=C30/(C29-C2)
      C36=C31/(C29-C3)
      C37=C32/(C29-C10)
      C38=C33/(C29-C20)
```

```
      C39=C30/(C2-C29)-C31/(C3-C29)+C32/(C10-C29)+C33/(C20-C29)+C34
      C40=CS133C*PHI
      C41=C29*C35
      C42=C28*C36
      C43=C28*C37
      C44=C28*C38
      C45=C28*C39
      C46=CS133I
      C47=C41/(C40-C2)
      C48=C42/(C40-C3)
      C49=C43/(C40-C10)
      C50=C44/(C40-C20)
      C51=C45/(C40-C29)
      C52=C41/(C2-C40)-C42/(C3-C40)+C43/(C10-C40)+C44/(C20-C40)+
     1C45/(C29-C40)+C46
      C53=YCS134*C14
      C54=CS133C*PHI
      C55=CS134C*PHI
      C56=DCS134
      C57=C54*C47
      C58=C54*C48
      C59=C54*C49
      C60=C54*C50
      C61=C54*C51
      C62=C54*C52
      C63=CS134I
      C64=C55+C56
      C65=C53+C57
      C66=C65/(C64-C2)
      C67=-C2*T
      C68=C58/(C64-C3)
      C69=-C3*T
      C70=C59/(C64-C10)
      C71=-C10*T
      C72=C60/(C64-C20)
      C73=-C20*T
      C74=C61/(C64-C29)
      C75=-C29*T
      C76=C62/(C64-C40)
      C77=-C40*T
      C78=C65/(C2-C64)-C58/(C3-C64)+C59/(C10-C64)+C60/(C20-C64)+
     1C61/(C29-C64)+C62/(C40-C64)+C63
      C79=-C64*T
      AMT134=C66*EXP(C67)-C68*EXP(C69)+C70*EXP(C71)+C72*EXP(C73)+
     1C74*EXP(C75)+C76*EXP(C77)+C78*EXP(C79)
      D1=C14
      D2=C2
      D3=YI137
      D4=D1*D3
      D5=DI137
      D6=I137I
      D7=D4/(D5-D2)
      D8=D6+D4/(D2-D5)
      D9=DXE137
      D10=D5*D7
      D11=D5*D3
      D12=XE137I
```

```
PROGRAM TEST        74/74   OPT=1                                FTN 4.6+446        08

      D13=D10/(D9-D2)
      D14=D11/(D9-D5)
      D15=D10/(D2-D3)+D11/(D5-D9)+D12
      D16=YCS137*D1
      D17=DCS137
      D18=D9*D13
      D19=D9*D14
      D20=D9*D15
      D21=D16+D18
      D22=CS137I
      D23=D21/(D2-D17)+D19/(D5-D17)+D20/(D9-D17)+D22
      D24=D20/(D17-D9)
      D25=D19/(D17-D5)
      D26=D21/(D17-D2)
      D27=-D2*T
      D28=-D5*T
      D29=-D9*T
      D30=-D17*T
      AMT137=D26*EXP(D27)+D25*EXP(D28)+D24*EXP(D29)+D23*EXP(D30)
      ACT134=AMT134*DCS134
      ACT137=AMT137*DCS137
      R=ACT134/ACT137
      PRINT*,"PHI=",PHI,"  T=",T,"   AMT134=",AMT134,"   AMT137=",AMT137
      U235I=U235I*EXP(-C2*T)
      PRINT*,"U235I=",U235I
      SB133I=C5*EXP(-C2*T)-C6*EXP(-C3*T)
      TE133I=C13*EXP(-C10*T)+C14*EXP(-C2*T)-C15*EXP(-C3*T)
      I133I=C23*EXP(-C2*T)-C24*EXP(-C3*T)+C25*EXP(-C10*T)+
     1C26*EXP(-C20*T)
      XE133I=C35*EXP(-C2*T)-C36*EXP(-C3*T)+C37*EXP(-C10*T)+
     1C38*EXP(-C20*T)+C39*EXP(-C29*T)
      CS133I=C47*EXP(-C2*T)-C46*EXP(-C3*T)+C49*EXP(-C10*T)+
     1C50*EXP(-C20*T)+C51*EXP(-C29*T)+C52*EXP(-C40*T)
      CS134I=AMT134
      I137I=D7*EXP(-D2*T)+D8*EXP(-D5*T)
      XE137I=D13*EXP(-D2*T)+D14*EXP(-D5*T)+D15*EXP(-D9*T)
      CS137I=AMT137
  101 CONTINUE
      STOP"END OF PROGRAM"
      END
```

PHI=2.58E+13 T=9504000. AMT134=15613.54278132 AMT137=808378.9137188
U235I=123421827.2363
PHI=2.58E+13 T=9504000. AMT134=61007.09069415 AMT137=1515457.695977
U235I=103606767.4168
PHI=2.63E+13 T=9504000. AMT134=129223.0384843 AMT137=2144651.409578
U235I=95688350.35563
PHI=2.71E+13 T=9504000. AMT134=215315.9192732 AMT137=2708360.659031
U235I=83323344.43414
PHI=2.81E+13 T=9504000. AMT134=315358.9269831 AMT137=3213868.312299
U235I=73071723.24519
PHI=2.93E+13 T=9504000. AMT134=426204.1643204 AMT137=3666777.531047
U235I=63326044.83113
PHI=3.05E+13 T=9504000. AMT134=544137.6154911 AMT137=4068316.037954
U235I=54560769.66557
PHI=3.18E+13 T=9504000. AMT134=666212.5866371 AMT137=4423405.501187
U235I=46710563.55466
PHI=3.31E+13 T=9504000. AMT134=789180.2450973 AMT137=4732803.049118
U235I=39736691.73048
PHI=3.45E+13 T=9504000. AMT134=910626.0885073 AMT137=5000517.907307
U235I=33573617.12123

```
PROGRAM YCSFOUR(INPUT,OUTPUT)
REAL I133I,I137I
DIMENSION INTEGR(6),ARRAY1(10),ARRAY2(10),ARRAY3(4,2)
DATA INTEGR/3*(-0),0,2*(-0)/
CALL SYSTEMC(113,INTEGR)
READ*,U235I,SIGF,SIGA
READ*,SB133I,YSB133,DSB133
READ*,TE133I,YTE133,DTE133
READ*,I133I,YI133,DI133
READ*,XE133I,XE133C,DXE133
READ*,CS133I,CS133C
READ*,I137I,YI137,DI137
READ*,XE137I,DXE137
READ*,CS137I,YCS137,DCS137,CS137C
READ*,ARRAY1,ARRAY2,ARRAY3
PRINT*,ARRAY1
PRINT*,ARRAY2
PRINT*,ARRAY3
DO 101 I=1,10
PHI=ARRAY1(I)
DO 101 J=1,10
T=ARRAY2(J)
DO 101 K=1,2
CS134I=ARRAY3(1,K)
YCS134=ARRAY3(2,K)
DCS134=ARRAY3(3,K)
CS134C=ARRAY3(4,K)
C1A=U235I*SIGF*PHI
C1=YSB133*C1A
C2=SIGA*PHI
C3=DSB133
C4=SB133I
C5=C1/(C3-C2)
C6=(C1+(C2*C4)-(C3*C4))/(C3-C2)
C7=YTE133*C1A
C8=C3*C5
C9=C3*C6
C10=DTE133
C11=C7+C8
C12=TE133I
C13=C11/(C2-C10)+C12-C9/(C3-C10)
C14=C11/(C10-C2)
C15=C9/(C10-C3)
C16=YI133*C1A
C17=C10*C13
C18=C10*C14
C19=C10*C15
C20=DI133
C21=C16+C18
C22=I133I
C23=C21/(C20-C2)
C24=C19/(C20-C3)
C25=C17/(C20-C10)
C26=C22+C17/(C10-C20)-C19/(C3-C20)
C27=XE133C*PHI
C28=DXE133
C29=C27+C28
```

AD-A066 200 AIR FORCE INST OF TECH WRIGHT-PATTERSON AFB OHIO SCH--ETC F/G 18/12
ISOTOPIC CORRELATION TECHNIQUES AS AN OFF-SITE REACTOR MONITOR.(U)
OCT 78 J L CLARK
UNCLASSIFIED AFIT/GNE/PH/78-12 NL

2 OF 2
AD
A066200

END
DATE
FILMED
5-79
DDC

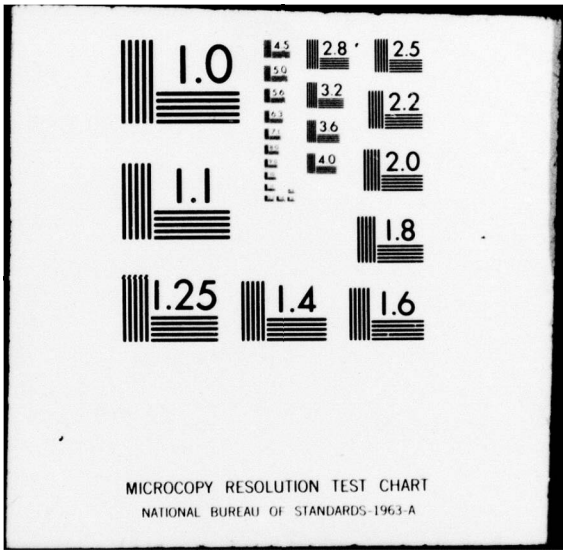
1.0
1.1
1.25
1.4
1.6
1.8
2.0
2.2
2.5
2.8
3.2
3.6
4.0
MICROCOPY RESOLUTION TEST CHART
NATIONAL BUREAU OF STANDARDS-1963-A

```
      C30=C20*C23
      C31=C20*C24
      C32=C20*C25
      C33=C20*C26
      C34=XF133I
      C35=C30/(C29-C2)
      C36=C31/(C29-C3)
      C37=C32/(C29-C10)
      C38=C33/(C29-C20)
      C39=C30/(C2-C29)-C31/(C3-C29)+C32/(C10-C29)+C33/(C20-C29)+C34
      C40=CS133C*PHI
      C41=C28*C35
      C42=C28*C36
      C43=C28*C37
      C44=C28*C38
      C45=C28*C39
      C46=CS133I
      C47=C41/(C40-C2)
      C48=C42/(C40-C3)
      C49=C43/(C40-C10)
      C50=C44/(C40-C20)
      C51=C45/(C40-C29)
      C52=C41/(C2-C40)-C42/(C3-C40)+C43/(C10-C40)+C44/(C20-C40)+
     1C45/(C29-C40)+C46
      C53=YCS134*C1A
      C54=CS133C*PHI
      C55=CS134C*PHI
      C56=DCS134
      C57=C54*C47
      C58=C54*C48
      C59=C54*C49
      C60=C54*C50
      C61=C54*C51
      C62=C54*C52
      C63=CS134I
      C64=C55+C56
      C65=C53+C57
      C66=C65/(C64-C2)
      C67=-C2*T
      C68=C58/(C64-C3)
      C69=-C3*T
      C70=C59/(C64-C10)
      C71=-C10*T
      C72=C60/(C64-C20)
      C73=-C20*T
      C74=C61/(C64-C29)
      C75=-C29*T
      C76=C62/(C64-C40)
      C77=-C40*T
      C78=C65/(C2-C64)-C53/(C3-C64)+C59/(C10-C64)+C60/(C20-C64)+
     1C61/(C29-C64)+C52/(C40-C64)+C63
      C79=-C64*T
      AMT134=C66*EXP(C67)-C68*EXP(C69)+C70*EXP(C71)+C72*EXP(C73)+
     1C74*EXP(C75)+C76*EXP(C77)+C78*EXP(C79)
      D1=C1A
      D2=C2
      D3=YI137
```

```
      D4=D1*D3
      D5=DI137
      D6=I137I
      D7=D4/(D5-D2)
      D8=D6+D4/(D2-D5)
      D9=DXE137
      D10=D5*D7
      D11=D5*D6
      D12=XE137I
      D13=D10/(D9-D2)
      D14=D11/(D9-D5)
      D15=D10/(D2-D9)+D11/(D5-D9)+D12
      D16=YCS137*D1
      D17=DCS137
      D18=D9*D13
      D19=D9*D14
      D20=D9*D15
      D21=D16+D18
      D22=CS137I
      D23=D21/(D2-D17)+D19/(D5-D17)+D20/(D9-D17)+D22
      D24=D20/(D17-D9)
      D25=D19/(D17-D5)
      D26=D21/(D17-D2)
      D27=-D2*T
      D28=-D5*T
      D29=-D9*T
      D30=-D17*T
      AMT137=D26*EXP(D27)+D25*EXP(D28)+D24*EXP(D29)+D23*EXP(D30)
      ACT134=AMT134*DCS134
      ACT137=AMT137*DCS137
      R=ACT134/ACT137
      PRINT*,"PHI=",PHI,"  T=",T,"  YCS134=",YCS134,"  AMT134=",AMT134,
     1"  R=",R
  101 CONTINUE
      STOP"END OF PROGRAM"
      END
```

```
1.E+13 2.E+13 3.E+13 4.E+13 5.E+13 6.E+13 7.E+13 8.E+13 9.E+13 1.E+14
2592000. 5184000. 7776000. 10370000. 12960000. 15550000. 18140000. 20740000. 2333
0. 0. 1.07E-8 1.07E-22 0. .0000052 1.07E-8 1.07E-22
PHI=1.E+13  T=2592000.  YCS134=0.  AMT134=134.085705041  R=.0216399566001
PHI=1.E+13  T=2592000.  YCS134=.0000052  AMT134=141.6362328073  R=.0225502392194
PHI=1.E+13  T=5184000.  YCS134=0.  AMT134=564.7618422134  R=.0540477403596
PHI=1.E+13  T=5184000.  YCS134=.0000052  AMT134=679.5757980852  R=.0652489543509
PHI=1.E+13  T=7776000.  YCS134=0.  AMT134=1539.756332661  R=.0873143954324
PHI=1.E+13  T=7776000.  YCS134=.0000052  AMT134=1620.432653107  R=.0884985528734
PHI=1.E+13  T=10370000.  YCS134=0.  AMT134=2319.154727737  R=.1204135491626
PHI=1.E+13  T=10370000.  YCS134=.0000052  AMT134=2946.445235274  R=.1215300172143
PHI=1.E+13  T=12960000.  YCS134=0.  AMT134=4500.561272244  R=.1530-94274835
PHI=1.E+13  T=12960000.  YCS134=.0000052  AMT134=4635.175332994  R=.1542002906333
PHI=1.E+13  T=15550000.  YCS134=0.  AMT134=6529.591926969  R=.1852059375773
PHI=1.E+13  T=15550000.  YCS134=.0000052  AMT134=6670.206175706  R=.1863-034734-
PHI=1.E+13  T=18140000.  YCS134=0.  AMT134=8357.049419537  R=.2165591255195
PHI=1.E+13  T=18140000.  YCS134=.0000052  AMT134=9074.009515974  R=.2179777263383
PHI=1.E+13  T=20740000.  YCS134=0.  AMT134=11561.77398923  R=.2481204956736
PHI=1.E+13  T=20740000.  YCS134=.0000052  AMT134=11720.60136373  R=.2492232731388
PHI=1.E+13  T=23330000.  YCS134=0.  AMT134=14635.83648877  R=.2787489710367
PHI=1.E+13  T=23330000.  YCS134=.0000052  AMT134=14892.97326712  R=.2798356221744
PHI=1.E+13  T=25920000.  YCS134=0.  AMT134=17483.1044735  R=.3086550727052
PHI=1.E+13  T=25920000.  YCS134=.0000052  AMT134=17945.15347373  R=.3099405301535
PHI=2.E+13  T=2592000.  YCS134=0.  AMT134=533.2047386688  R=.0437133739597
PHI=2.E+13  T=2592000.  YCS134=.0000052  AMT134=546.1845833382  R=.0447021962303
PHI=2.E+13  T=5184000.  YCS134=0.  AMT134=2575.769794165  R=.1081655957206
PHI=2.E+13  T=5184000.  YCS134=.0000052  AMT134=2654.345277259  R=.1093632209625
PHI=2.E+13  T=7776000.  YCS134=0.  AMT134=5272.146402633  R=.1746998166367
PHI=2.E+13  T=7776000.  YCS134=.0000052  AMT134=6314.472588157  R=.1753777327604
PHI=2.E+13  T=10370000.  YCS134=0.  AMT134=11370.25087813  R=.2403471223308
```

```
PHI=2.E+13  T=10370010.  YCS134=.0000052  AMT134=11425.07933902  R=.2420074632295
PHI=2.E+13  T=12960100.  YCS134=0.  AMT134=17607.30435277  R=.3000105309434
PHI=2.E+13  T=12960100.  YCS134=.0000052  AMT134=17769.7466[illegible]  R=.3071525685415
PHI=2.E+13  T=13550100.  YCS134=0.  AMT134=20470.86949707  R=.3701403954393
PHI=2.E+13  T=13550000.  YCS134=.0000052  AMT134=25557.24017566  R=.4712733680001
PHI=2.E+13  T=18140100.  YCS134=0.  AMT134=34396.50622023  R=.4332068927086
PHI=2.E+13  T=18140000.  YCS134=.0000052  AMT134=34394.10740136  R=.4734150696775
PHI=2.E+13  T=20740100.  YCS134=0.  AMT134=44274.4098583  R=.4954042179144
PHI=2.E+13  T=20740000.  YCS134=.0000052  AMT134=44331.85351111  R=.4986976950379
PHI=2.E+13  T=23330000.  YCS134=0.  AMT134=55102.64226141  R=.5562494434136
PHI=2.E+13  T=23330100.  YCS134=.0000052  AMT134=55206.74755349  R=.5573205540491
PHI=2.E+13  T=25920100.  YCS134=0.  AMT134=65866.95474293  R=.6153663787906
PHI=2.E+13  T=25920000.  YCS134=.0000052  AMT134=66081.35517943  R=.6173584499207
PHI=3.E+13  T=2592000.  YCS134=0.  AMT134=1132.095608592  R=.0850139897316
PHI=3.E+13  T=2592000.  YCS134=.0000052  AMT134=1214.956743297  R=.0882470379126
PHI=3.E+13  T=5184000.  YCS134=0.  AMT134=5834.153341327  R=.1623459601[illegible]5
PHI=3.E+13  T=5184000.  YCS134=.0000052  AMT134=5877.069932058  R=.1635412007973
PHI=3.E+13  T=7776000.  YCS134=0.  AMT134=13341.74912344  R=.2621294981352
PHI=3.E+13  T=7776000.  YCS134=.0000052  AMT134=13903.72317658  R=.2733131379189
PHI=3.E+13  T=10370000.  YCS134=0.  AMT134=24927.27341133  R=.3612429810952
PHI=3.E+13  T=10370000.  YCS134=.0000052  AMT134=25001.87555135  R=.3623962354633
PHI=3.E+13  T=12960100.  YCS134=0.  AMT134=37758.22832904  R=.4587696756163
PHI=3.E+13  T=12960100.  YCS134=.0000052  AMT134=38533.95799813  R=.4599027397717
PHI=3.E+13  T=13550000.  YCS134=0.  AMT134=53094.3455012[illegible]  R=.5548339154065
PHI=3.E+13  T=13550000.  YCS134=.0000052  AMT134=55204.93523541  R=.5597471299402
PHI=3.E+13  T=18140100.  YCS134=0.  AMT134=73577.43003077  R=.6497384926536
PHI=3.E+13  T=18140000.  YCS134=.0000052  AMT134=73801.6325341  R=.6498320190741
PHI=3.E+13  T=20740000.  YCS134=0.  AMT134=94357.68102843  R=.7413890060944
PHI=3.E+13  T=20740000.  YCS134=.0000052  AMT134=94430.36258291  R=.7424537006[illegible]49
PHI=3.E+13  T=23330100.  YCS134=0.  AMT134=116741.2754724  R=.8718484294377
PHI=3.E+13  T=23330000.  YCS134=.0000052  AMT134=116389.7373926  R=.8329031703716
PHI=3.E+13  T=25920100.  YCS134=0.  AMT134=140708.5862136  R=.9204535110[illegible]8
PHI=3.E+13  T=25920000.  YCS134=.0000052  AMT134=140866.9135954  R=.9214983303535
PHI=4.E+13  T=2592000.  YCS134=0.  AMT134=2137.962384356  R=.0887579777152
PHI=4.E+13  T=2592000.  YCS134=.0000052  AMT134=2137.447006235  R=.0879717[illegible]1476
PHI=4.E+13  T=5184000.  YCS134=0.  AMT134=10342.40326651  R=.2165352384479
PHI=4.E+13  T=5184000.  YCS134=.0000052  AMT134=10258.71755786  R=.2177759723902
PHI=4.E+13  T=7776000.  YCS134=0.  AMT134=24136.76161951  R=.3495825104628
PHI=4.E+13  T=7776000.  YCS134=.0000052  AMT134=24217.42833995  R=.3507509396197
PHI=4.E+13  T=10370000.  YCS134=0.  AMT134=43165.16590691  R=.4815473090002
PHI=4.E+13  T=10370000.  YCS134=.0000052  AMT134=43267.80233231  R=.4826594162282
PHI=4.E+13  T=12960000.  YCS134=0.  AMT134=66574.796756  R=.5112132706037
PHI=4.E+13  T=12960100.  YCS134=.0000052  AMT134=66799.4357326[illegible]  R=.5123373958173
PHI=4.E+13  T=13550100.  YCS134=0.  AMT134=94147.02952973  R=.7384535433244
PHI=4.E+13  T=13550000.  YCS134=.0000052  AMT134=94283.53152814  R=.7395058854931
PHI=4.E+13  T=18140100.  YCS134=0.  AMT134=125052.5953113  R=.9631335177503
PHI=4.E+13  T=18140100.  YCS134=.0000052  AMT134=125209.1539032  R=.9642192828134
PHI=4.E+13  T=20740000.  YCS134=0.  AMT134=159070.3013116  R=.9855157841671
PHI=4.E+13  T=20740000.  YCS134=.0000052  AMT134=159241.2550784  R=.9865761043693
PHI=4.E+13  T=23330000.  YCS134=0.  AMT134=135499.4785041  R=1.104900542548
PHI=4.E+13  T=23330100.  YCS134=.0000052  AMT134=135683.1503938  R=1.105938707549
PHI=4.E+13  T=25920100.  YCS134=0.  AMT134=234046.9495729  R=1.221427625506
PHI=4.E+13  T=25920000.  YCS134=.0000052  AMT134=234261.8839116  R=1.222444358586
PHI=5.E+13  T=2592000.  YCS134=0.  AMT134=3274.463954606  R=.1085279006335
PHI=5.E+13  T=2592000.  YCS134=.0000052  AMT134=3311.021034003  R=.1047395400489
PHI=5.E+13  T=5184000.  YCS134=0.  AMT134=15304.33643453  R=.2708738060877
PHI=5.E+13  T=5184000.  YCS134=.0000052  AMT134=15473.60719372  R=.2720510174565
PHI=5.E+13  T=7776000.  YCS134=0.  AMT134=36333.70277732  R=.4370342793277
PHI=5.E+13  T=7776000.  YCS134=.0000052  AMT134=37092.14613395  R=.4351372649292
PHI=5.E+13  T=10370000.  YCS134=0.  AMT134=65713.52174838  R=.6015902919521
PHI=5.E+13  T=10370000.  YCS134=.0000052  AMT134=65837.91063745  R=.6026252015837
PHI=5.E+13  T=12960000.  YCS134=0.  AMT134=100877.8097201  R=.7632250234379
PHI=5.E+13  T=12960100.  YCS134=.0000052  AMT134=100975.1131177  R=.7647430[illegible]114
PHI=5.E+13  T=13550000.  YCS134=0.  AMT134=141412.4034003  R=.9214434725686
PHI=5.E+13  T=13550100.  YCS134=.0000052  AMT134=141579.[illegible]489514  R=.9227[illegible]634804
PHI=5.E+13  T=18140000.  YCS134=0.  AMT134=145503.6104679  R=1.075102681477
```

```
PHI=5.E+13  T=1814.0000.  YCS134=.0000052  AMT134=196778.7753448  R=1.077170330287
PHI=5.E+13  T=2074.0000.  YCS134=0.  AMT134=235775.0560173  R=1.227835431997
PHI=5.E+13  T=2074.0000.  YCS134=.0000052  AMT134=235975.4552024  R=1.228079370701
PHI=5.E+13  T=2331.0000.  YCS134=0.  AMT134=237860.1900055  R=1.237477203226
PHI=5.E+13  T=2333.0000.  YCS134=.0000052  AMT134=238074.0595501  R=1.375798113601
PHI=5.E+13  T=2592.0000.  YCS134=0.  AMT134=342383.1376657  R=1.518032270151
PHI=5.E+13  T=2592.0000.  YCS134=.0000052  AMT134=342510.3553097  R=1.518288238143
PHI=6.E+13  T=2592.0000.  YCS134=0.  AMT134=4687.723280603  R=1.130328719296?
PHI=6.E+13  T=2592.0000.  YCS134=.0000052  AMT134=4731.241752148  R=1.131578551496096
PHI=6.E+13  T=5184.0000.  YCS134=0.  AMT134=22475.07152?6  R=.3252051200549
PHI=6.E+13  T=5184.0000.  YCS134=.0000052  AMT134=22556.8733857  R=.326330?932564
PHI=6.E+13  T=7776.0000.  YCS134=0.  AMT134=52256.12797032  R=.524460594?736
PHI=6.E+13  T=7776.0000.  YCS134=.0000052  AMT134=52371.46665214  R=.526161263223
PHI=6.E+13  T=10370.000.  YCS134=0.  AMT134=92200.3594?513  R=.721625203?792
PHI=6.E+13  T=10370.000.  YCS134=.0000052  AMT134=92348.9545?843  R=.722757855?735
PHI=6.E+13  T=12960.000.  YCS134=0.  AMT134=140573.651453  R=.914701227?122
PHI=6.E+13  T=12960.000.  YCS134=.0000052  AMT134=140703.5583446  R=.915607119?048
PHI=6.E+13  T=15550.000.  YCS134=0.  AMT134=195796.466281  R=1.107340?78535
PHI=6.E+13  T=15550.000.  YCS134=.0000052  AMT134=195988.1575372  R=1.104460959093
PHI=6.E+13  T=18140.000.  YCS134=0.  AMT134=256652.8614153  R=1.267?289959
PHI=6.E+13  T=18140.000.  YCS134=.0000052  AMT134=256853.1541787  R=1.268?63?44355
PHI=6.E+13  T=20730.000.  YCS134=0.  AMT134=322165.3713603  R=1.46?00236?77
PHI=6.E+13  T=20730.000.  YCS134=.0000052  AMT134=322395.?230578  R=1.46?8031?80665
PHI=6.E+13  T=23320.000.  YCS134=0.  AMT134=390778.258607  R=1.64?848692504
PHI=6.E+13  T=23320.000.  YCS134=.0000052  AMT134=391017.?929572  R=1.64?6?3175085
PHI=6.E+13  T=25920.000.  YCS134=0.  AMT134=461737.55?0?63  R=1.809432932?99
PHI=6.E+13  T=25920.000.  YCS134=.0000052  AMT134=462037.5856097  R=1.810?12617434
PHI=7.E+13  T=2592.000.  YCS134=0.  AMT134=5343.721665912  R=.152159791377?
PHI=7.E+13  T=2592.000.  YCS134=.0000052  AMT134=5393.687?35277  R=.153367?391093
PHI=7.E+13  T=5184.000.  YCS134=0.  AMT134=30210.976?2848  R=.379?752215?23
PHI=7.E+13  T=5184.000.  YCS134=.0000052  AMT134=30304.90?05199  R=.380?5?3411027
PHI=7.E+13  T=7776.000.  YCS134=0.  AMT134=69774.354?5027  R=.51163759223?5
PHI=7.E+13  T=7776.000.  YCS134=.0000052  AMT134=69905.75?15936  R=.512989?914257
PHI=7.E+13  T=10370.000.  YCS134=0.  AMT134=122205.9156593  R=.841233516?637
PHI=7.E+13  T=10370.000.  YCS134=.0000052  AMT134=122459.?5?5308  R=.842417?659951
PHI=7.E+13  T=12960.000.  YCS134=0.  AMT134=135166.7575611  R=1.0655?09?4?033
PHI=7.E+13  T=12960.000.  YCS134=.0000052  AMT134=185357.3354318  R=1.066617603411
PHI=7.E+13  T=15550.000.  YCS134=0.  AMT134=255287.7757313  R=1.284?94542339
PHI=7.E+13  T=15550.000.  YCS134=.0000052  AMT134=256501.1551031  R=1.285153646925
PHI=7.E+13  T=18140.000.  YCS134=0.  AMT134=333795.490123  R=1.49652116931
PHI=7.E+13  T=18140.000.  YCS134=.0000052  AMT134=333957.9143508  R=1.497562631168
PHI=7.E+13  T=20730.000.  YCS134=0.  AMT134=?162?0.3574792  R=1.703?96094024
PHI=7.E+13  T=20730.000.  YCS134=.0000052  AMT134=416478.?432123  R=1.704?00505469
PHI=7.E+13  T=23320.000.  YCS134=0.  AMT13?=501624.3694931  R=1.90253333?056
PHI=7.E+13  T=23320.000.  YCS134=.0000052  AMT134=501884.?154259  R=1.90?320820531
PHI=7.E+13  T=25920.000.  YCS134=0.  AMT134=588900.0134617  R=2.0946?297?308
PHI=7.E+13  T=25920.000.  YCS134=.0000052  AMT134=589260.1200137  R=2.095?23?66217
PHI=8.E+13  T=2592.000.  YCS134=0.  AMT134=8234.899032727  R=.174020472?917
PHI=8.E+13  T=2592.000.  YCS134=.0000052  AMT134=8294.001?72613  R=.175225?691383
PHI=8.E+13  T=5184.000.  YCS134=0.  AMT134=38359.?5550636  R=.433974?330139
PHI=8.E+13  T=5184.000.  YCS134=.0000052  AMT134=39075.?0?30504  R=.435151?897757
PHI=8.E+13  T=7776.000.  YCS134=0.  AMT134=89405.19?59?08  R=.699141643?805
PHI=8.E+13  T=7776.000.  YCS134=.0000052  AMT134=89551.8?75569  R=.700?834027029
PHI=8.E+13  T=10370.000.  YCS134=0.  AMT134=155606.55?8198?  R=.95?6?4919?903
PHI=8.E+13  T=10370.000.  YCS134=.0000052  AMT134=155847.5822177  R=.961751?150912
PHI=8.E+13  T=12960.000.  YCS134=0.  AMT134=234146.?067605  R=1.215576?51669
PHI=8.E+13  T=12960.000.  YCS134=.0000052  AMT134=234395.?55517?  R=1.215663?10619
PHI=8.E+13  T=15550.000.  YCS134=0.  AMT134=?219?9.97?645  R=1.463?57?56497
PHI=8.E+13  T=15550.000.  YCS134=.0000052  AMT134=?22202.0?57722  R=1.464?25297824
PHI=8.E+13  T=18140.000.  YCS134=0.  AMT134=415?13.4?51?6?  R=1.703?89?04377
PHI=8.E+13  T=18140.000.  YCS134=.0000052  AMT134=416834.?6?5?08  R=1.70?418?94172
PHI=8.E+13  T=20730.000.  YCS134=0.  AMT134=516195.?04708  R=1.93?059?95935
PHI=8.E+13  T=20730.000.  YCS134=.0000052  AMT134=516452.?059495  R=1.937?6?39624?
PHI=8.E+13  T=23320.000.  YCS134=0.  AMT134=616175.?18463?  R=2.15?2?6?13925
PHI=8.E+13  T=23320.000.  YCS134=.0000052  AMT134=616412.0?77748  R=2.15?227?7745?
PHI=8.E+13  T=25920.000.  YCS134=0.  AMT134=?21?71.1?20634  R=2.37?57?06154
```

```
PHI=8.E+13  T=25920000.  YCS134=.0000052  AMT134=721507.7364593  R=2.3745116650412
PHI=9.E+13  T=25920000.  YCS134=0.  AMT134=10364.1732059  R=.1395101167382
PHI=9.E+13  T=25920000.  YCS134=.0000052  AMT134=10427.881775631  R=.1971147561667
PHI=9.E+13  T=51840000.  YCS134=0.  AMT134=8709.90321952  R=.4383972850074
PHI=9.E+13  T=51840000.  YCS134=.0000052  AMT134=46826.64738022  R=.4389704526991
PHI=9.E+13  T=77760000.  YCS134=0.  AMT134=111011.7162558  R=.7863486034125
PHI=9.E+13  T=77760000.  YCS134=.0000052  AMT134=111172.8351546  R=.7874496971013
PHI=9.E+13  T=103680000.  YCS134=0.  AMT134=132013.710293  R=1.0795934776896
PHI=9.E+13  T=103680000.  YCS134=.0000052  AMT134=192211.153354  R=1.0807033067251
PHI=9.E+13  T=129600000.  YCS134=0.  AMT134=269975.1730789  R=1.3648579187917
PHI=9.E+13  T=129600000.  YCS134=.0000052  AMT134=287161.7571507  R=1.3683359099391
PHI=9.E+13  T=155520000.  YCS134=0.  AMT134=332010.2624012  R=1.5410453413072
PHI=9.E+13  T=155520000.  YCS134=.0000052  AMT134=392260.7680965  R=1.6420691910922
PHI=9.E+13  T=181440000.  YCS134=0.  AMT134=503960.2067657  R=1.9076531229517
PHI=9.E+13  T=181440000.  YCS134=.0000052  AMT134=504228.0883892  R=1.9086827655844
PHI=9.E+13  T=207360000.  YCS134=0.  AMT134=620402.794902  R=2.1649502738353
PHI=9.E+13  T=207360000.  YCS134=.0000052  AMT134=620764.7824568  R=2.1663434132452
PHI=9.E+13  T=233280000.  YCS134=0.  AMT134=738359.5626356  R=2.4104777730226
PHI=9.E+13  T=233280000.  YCS134=.0000052  AMT134=738661.4462091  R=2.4114307360568
PHI=9.E+13  T=259200000.  YCS134=0.  AMT134=876153.7601391  R=2.6483567755073
PHI=9.E+13  T=259200000.  YCS134=.0000052  AMT134=876532.3513721  R=2.6497751436035
PHI=1.E+14  T=25920000.  YCS134=0.  AMT134=10720.83920892  R=.2178280765061
PHI=1.E+14  T=25920000.  YCS134=.0000052  AMT134=12791.06558539  R=.2193309547316
PHI=1.E+14  T=51840000.  YCS134=0.  AMT134=59391.70098243  R=.5428379733591
PHI=1.E+14  T=51840000.  YCS134=.0000052  AMT134=59519.64113591  R=.5440073418715
PHI=1.E+14  T=77760000.  YCS134=0.  AMT134=134462.9661429  R=.8734347868443
PHI=1.E+14  T=77760000.  YCS134=.0000052  AMT134=134637.3139119  R=.8745705755975
PHI=1.E+14  T=103680000.  YCS134=0.  AMT134=231052.3470096  R=1.1991126577725
PHI=1.E+14  T=103680000.  YCS134=.0000052  AMT134=231265.7321179  R=1.1997147994457
PHI=1.E+14  T=129600000.  YCS134=0.  AMT134=343076.7752985  R=1.5129575615554
PHI=1.E+14  T=129600000.  YCS134=.0000052  AMT134=343279.0543503  R=1.5140262233537
PHI=1.E+14  T=155520000.  YCS134=0.  AMT134=465653.0967079  R=1.8159385653334
PHI=1.E+14  T=155520000.  YCS134=.0000052  AMT134=465918.3718314  R=1.8179736473777
PHI=1.E+14  T=181440000.  YCS134=0.  AMT134=594840.5314627  R=2.1030795562004
PHI=1.E+14  T=181440000.  YCS134=.0000052  AMT134=595127.0582725  R=2.1100413177+1
PHI=1.E+14  T=207360000.  YCS134=0.  AMT134=727707.1063179  R=2.3835455279926
PHI=1.E+14  T=207360000.  YCS134=.0000052  AMT134=725062.0792295  R=2.3905143394256
PHI=1.E+14  T=233280000.  YCS134=0.  AMT134=856869.1637847  R=2.8555863+9931
PHI=1.E+14  T=233280000.  YCS134=.0000052  AMT134=860972.4051593  R=2.856622571343
PHI=1.E+14  T=259200000.  YCS134=0.  AMT134=9819[illegible]5.0459887  R=2.903078192479
PHI=1.E+14  T=259200000.  YCS134=.0000052  AMT134=992153.1317[illegible]  R=2.903981399721

ERROR SUMMARY
    ERROR      TIMES
     0115       0[illegible]00
```

SECURITY CLASSIFICATION OF THIS PAGE (When Data Entered)

REPORT DOCUMENTATION PAGE

READ INSTRUCTIONS BEFORE COMPLETING FORM

1. REPORT NUMBER: AFIT/GNE/PH/78D-12	2. GOVT ACCESSION NO.
3. RECIPIENT'S CATALOG NUMBER	
4. TITLE (and Subtitle): ISOTOPIC CORRELATION TECHNIQUES AS AN OFF-SITE REACTOR MONITOR	5. TYPE OF REPORT & PERIOD COVERED: MS Thesis
	6. PERFORMING ORG. REPORT NUMBER
7. AUTHOR(s): James L. Clark, Jr.	8. CONTRACT OR GRANT NUMBER(s)
9. PERFORMING ORGANIZATION NAME AND ADDRESS: Air Force Institute of Technology (AFIT/EN) Wright-Patterson AFB, Ohio 45433	10. PROGRAM ELEMENT, PROJECT, TASK AREA & WORK UNIT NUMBERS
11. CONTROLLING OFFICE NAME AND ADDRESS	12. REPORT DATE: October 1978
	13. NUMBER OF PAGES: 101
14. MONITORING AGENCY NAME & ADDRESS(if different from Controlling Office)	15. SECURITY CLASS. (of this report): Unclassified
	15a. DECLASSIFICATION/DOWNGRADING SCHEDULE

16. DISTRIBUTION STATEMENT (of this Report)

Approved for public release; distribution unlimited.

17. DISTRIBUTION STATEMENT (of the abstract entered in Block 20, if different from Report)

18. SUPPLEMENTARY NOTES

Approved for public release; IAW AFR 190-17

JOSEPH P. HIPPS, Major, USAF
Director of Information

FEB 8 1979

19. KEY WORDS (Continue on reverse side if necessary and identify by block number)

Isotopic Correlations
Cesium 134
Cesium 137
Neodymium

20. ABSTRACT (Continue on reverse side if necessary and identify by block number)

The feasibility of using the mass ratio Nd146/Nd145 and the activity ratio Cs134/Cs137 as off-site indicators of bomb-grade plutonium production in commercial light water reactors is examined. The theoretical basis of these ratios as on-site indicators of fluence is developed and experimental validation of their utility as such is examined. The escape rate of cesium and neodymium is approximated and detection limits determined. Although both ratios are experimentally validated as indicators of fluence, neither

(Continued on Reverse)

DD FORM 1 JAN 73 1473 EDITION OF 1 NOV 65 IS OBSOLETE

UNCLASSIFIED

SECURITY CLASSIFICATION OF THIS PAGE (When Data Entered)

BLOCK 20 (Continued):

cesium nor neodymium escapes a reactor in great enough concentration to be accurately measured off-site.